

One-Electron Singular Spectral Features of the 1D Hubbard Model

J. M. P. Carmelo

*Department of Physics, Massachusetts Institute of Technology, Cambridge, Massachusetts 02139-4307 and
GCEP-Center of Physics, University of Minho, Campus Gualtar, P-4710-057 Braga, Portugal*

K. Penc

Research Institute for Solid State Physics and Optics, H-1525 Budapest, P.O.B. 49, Hungary

P. D. Sacramento

Departamento de Física and CFIF, Instituto Superior Técnico, P-1049-001 Lisboa, Portugal

D. Bozi

Department of Physics and GCEP-CF, University of Minho, Campus Gualtar, P-4710-057 Braga, Portugal

R. Claessen

Experimentalphysik II, Universität Augsburg, D-86135 Augsburg, Germany

(Dated: 28 July 2003)

In this paper we use the pseudofermion dynamical theory (PDT) in the study of the one-electron spectral function of the one-dimensional Hubbard model. The PDT reveals that in the whole (k, ω) -plane the singular spectral features are of power-law type and correspond to well defined lines. Moreover, most of these lines correspond to two types of independent features: the charge and spin singular branch lines. One our goals is the study of the momentum and energy dependence of the spectral-weight distribution in the vicinity of such lines. Our expressions refer to all values of the electronic density and on-site repulsion U . The weight distribution in the vicinity of the branch lines is fully controlled by the overall pseudofermion phase shifts. Moreover, the shape of these lines is determined by the bare-momentum dependence of the pseudofermion energy dispersions. For suitable values of the on-site Coulombian repulsion and electronic density the theoretically predicted singular spectral features agree quantitatively for the whole momentum and energy bandwidth with the TCNQ peak dispersions observed by angle-resolved photoelectron spectroscopy in the quasi-1D organic conductor TTF-TCNQ.

PACS numbers: 71.20.-b, 71.10.Pm, 72.15.Nj, 71.27.+a

I. INTRODUCTION

The study of the microscopic mechanisms behind the unusual finite-energy spectral properties observed in quasi one-dimensional (1D) metals [1, 2, 3, 4] remains until now an interesting open problem. Indeed, the finite-energy spectral dispersions recently observed in such metals by angle-resolved photoelectron spectroscopy (ARPES) reveal significant discrepancies from the conventional band-structure description [1, 2, 3, 4].

There is some evidence that the electronic correlation effects described by the one-dimensional (1D) Hubbard model [5, 6] could contain the finite-energy microscopic mechanisms [1, 4] that control the above finite-energy spectral properties of that model. This is in contrast to simpler models [7]. Unfortunately, usual techniques such as bosonization [8] and conformal-field theory [9] do not apply at finite energy. Valuable qualitative information can be obtained for $U \rightarrow \infty$ by use of the method of Refs. [10, 11, 12]. However, a quantitative description of the finite-energy spectral properties of quasi-1D metals requires the solution of the problem for finite values of the on-site Coulombian repulsion U . The method of Ref. [13] refers to features of the insulator phase. For $U \approx 4t$, where t is the transfer integral, there are numerical results for the one-electron spectral function [14]. Unfortunately, the latter results provide very little information about the microscopic mechanisms behind the finite-energy spectral properties.

Recently, the preliminary use of the finite-energy holon and spinon representation introduced in Refs. [15, 16] and of the related pseudofermion description of Refs. [17, 18, 19, 21], revealed that most singular features of the one-electron spectral function correspond to separate charge and spin branch lines [4]. For the one-electron removal spectral function these lines show quantitative agreement with the TCNQ peak dispersions observed by ARPES in the quasi-1D organic conductor TTF-TCNQ [1, 2, 3]. However, these studies provide no information about the momentum and energy dependence of the spectral-weight distribution in the vicinity of the charge and spin branch lines. A preliminary exact study of that dependence was recently presented in Ref. [22]. Shortly after a study of the same problem by means of the dynamical density matrix renormalization group (DDMRG) method led to very similar

results [23]. The main goal of this paper is to extend the preliminary results of Ref. [22] by providing a detailed description of the evaluation of the one-electron spectral weight distribution in the vicinity of the singular features for all values of U and electronic density. In Ref. [24] the PDT is combined with the renormalization group for the study of the microscopic mechanisms behind the phase diagram observed in the (TMTTF)₂X and (TMTSF)₂X series of quasi-1D organic compounds. These studies are consistent with the latter phase diagram and explain why there are no superconducting phases in TTF-TCNQ.

The paper is organized as follows: In Sec. I we introduce the one-electron spectral-function problem, the 1D Hubbard model, and some basic information about the PDT. The general branch-line expression, the behavior at the branch-line end points, and the study of the quantities needed for the evaluation of the weight distribution in the vicinity of the one-electron spectral-function branch lines are the subjects of Sec. II. The study of the latter problem for both one-electron removal and addition is the topic of Sec. III. In Sec. IV we investigate the limiting behavior of the phase shifts and associated spectral-function behavior in the vicinity of the branch lines both for $U/t \rightarrow 0$ and $U/t \rightarrow \infty$. The relation of our theoretical predictions to the TCNQ branch lines observed by angle-resolved photoelectron spectroscopy in the quasi-1D organic compound TTF-TCNQ is discussed Sec. V. Finally, the concluding remarks are presented in Sec. VI.

A. THE MODEL AND THE ONE-ELECTRON SPECTRAL FUNCTIONS

The 1D Hubbard model reads,

$$\hat{H} = -t \sum_{j,\sigma} [c_{j,\sigma}^\dagger c_{j+1,\sigma} + h.c.] + U \sum_j \hat{n}_{j,\uparrow} \hat{n}_{j,\downarrow}, \quad (1)$$

where $c_{j,\sigma}^\dagger$ and $c_{j,\sigma}$ are spin-projection $\sigma = \uparrow, \downarrow$ electron operators at site $j = 1, 2, \dots, N_a$ and $\hat{n}_{j,\sigma} = c_{j,\sigma}^\dagger c_{j,\sigma}$. The model (1) describes N_\uparrow spin-up electrons and N_\downarrow spin-down electrons in a chain of N_a sites. We denote the electronic number by $N = N_\uparrow + N_\downarrow$. The number of lattice sites N_a is even and very large. For simplicity, we use units such that both the lattice spacing and the Planck constant are one. In these units the chain length L is such that $L = N_a$. Our results refer to periodic boundary conditions. We consider an electronic density $n = n_\uparrow + n_\downarrow$ in the range $0 < n < 1$ and a spin density $m = n_\uparrow - n_\downarrow$ such that $m \rightarrow 0$, where $n_\sigma = N_\sigma/L$ and $\sigma = \uparrow, \downarrow$. However, the calculations are fulfilled for finite values of the spin density m . The limit $m \rightarrow 0$ is taken in the end of the calculation and leads to the correct $m = 0$ results. The Fermi momentum is $k_F = \pi n/2$ and the electronic charge reads $-e$.

The one-electron spectral function $B^l(k, \omega)$ such that $l = -1$ (and $l = +1$) for electron removal (and addition) is given by,

$$\begin{aligned} B^{-1}(k, \omega) &= \sum_{\sigma} \sum_f |\langle f | c_{k,\sigma} | GS \rangle|^2 \delta(\omega + E_{f, N-1} - E_{GS}), \quad \omega < 0; \\ B^{+1}(k, \omega) &= \sum_{\sigma} \sum_{f'} |\langle f' | c_{k,\sigma}^\dagger | GS \rangle|^2 \delta(\omega - E_{f', N+1} + E_{GS}), \quad \omega > 0. \end{aligned} \quad (2)$$

Here $c_{k,\sigma}$ (and $c_{k,\sigma}^\dagger$) are electron annihilation (and creation) operators of momentum k and $|GS\rangle$ denotes the initial N -electron ground state. The f and f' summations run over the $N-1$ and $N+1$ -electron excited energy eigenstates, respectively, and $[E_{f, N-1} - E_{GS}]$ and $[E_{f', N+1} - E_{GS}]$ are the corresponding excitation energies. In this paper we use a momentum extended scheme such that $k \in (-\infty, +\infty)$ for the expressions given in Eq. (2), yet it is a simple exercise to obtain the corresponding spectral function expressions for the first Brillouin zone.

B. THE PSEUDOFERMION DYNAMICAL THEORY: DOMINANT PROCESSES FOR THE ONE-ELECTRON SPECTRAL WEIGHT

In this paper we apply the PDT introduced in Refs. [18, 19] to the study of the momentum and energy dependence of the spectral-weight distribution in the vicinity of the one-electron charge and spin branch lines. The PDT provides the expressions for the finite-number-electron spectral functions for all values of energy and momentum. The pseudofermion theory refers to the *pseudofermion subspace* (PS) defined in Ref. [17]. The one-electron excitations studied in this paper are contained in such a Hilbert subspace.

The one-electron spectral-weight distribution in the vicinity of the branch lines studied in Sec. III involves only the dominant processes defined in Refs. [18, 19]. The dominant (and non-dominant) processes correspond to the $i = 0$ (and $i > 0$) terms on the right-hand side of the general spectral-function expression given in Eq. (36) of Ref. [18], as discussed in Refs. [18, 19]. According to the PDT, such dominant processes generate excited energy eigenstates whose quantum-object number deviations obey the relation (41) of Ref. [18]. In reference [25] the dominant character of these processes is confirmed for the one-electron spectral functions studied here. Furthermore, only such dominant processes contribute to the one-electron spectral-function power-law expressions obtained in this paper, which are exact. Indeed, for the weight distribution in the vicinity of the above-mentioned branch lines the non-dominant processes give no finite contributions [19]. Moreover, the singular branch lines studied here have physical significance because they correspond to singular features of the one-electron spectral functions which can be observed in real materials [4, 22], as confirmed in Sec. V.

The general pseudofermion theory [15, 16, 17, 18, 19, 21] involves $c\nu$ pseudofermion branches such that $\nu = 0, 1, 2, \dots$ and $s\nu$ pseudofermion branches where $\nu = 1, 2, \dots$. However, most of our study refers to the three branches that contribute to the one-electron dominant processes, yet in some cases we provide general expressions that include all pseudofermion branches. For one-electron removal and addition spectral functions corresponding to densities $0 < n < 1$ and $m \rightarrow 0$ the above-mentioned dominant processes involve the $c0$ pseudofermions, $s1$ pseudofermions, and $c1$ pseudofermions of Refs. [17, 18], whereas the $n = 1$ problem involves the $-1/2$ Yang holons instead of the $c1$ pseudofermions. (The pseudofermions are related to the pseudoparticles studied in Refs. [15, 16] by a canonical transformation studied in Ref. [17].) Most of our final expressions refer to densities $0 < n < 1$ and $m \rightarrow 0$ and thus only involve the occupancy configurations of the above $c0$ pseudofermions, $s1$ pseudofermions, and $c1$ pseudofermions. According to the studies of Refs. [15, 16, 17], the $c0$ pseudofermion carries charge $-e$ and has no spin and the $s1$ pseudofermion is a spin-zero two-spinon composite object and has no charge. The $c1$ pseudofermion is a η -spin-zero two-holon composite object, carries charge $-2e$, and has spin zero. The $-1/2$ Yang holon has η -spin $1/2$, η -spin projection $-1/2$, charge $-2e$, and zero spin. (These charge values correspond to the description of the transport of charge in terms of electrons [15].) An important point that follows from the above analysis is that while the $c0$ and $c1$ pseudofermion branches are associated with excitations of charge character, the $s1$ pseudofermion branch describes spin excitations. The $c0$, $s1$, and $c1$ pseudofermions carry canonical-momentum $\bar{q} = q + Q_{\alpha\nu}^{\Phi}(q)/L$, where in our case $\alpha\nu = c0, s1, c1$. Here q is the *bare-momentum* and $Q_{\alpha\nu}^{\Phi}(q)/2$ is the overall scattering phase shift given by [17, 21],

$$Q_{\alpha\nu}^{\Phi}(q)/2 = \pi \sum_{\alpha'\nu'=c0, s1, c1} \sum_{q'} \Phi_{\alpha\nu, \alpha'\nu'}(q, q') \Delta N_{\alpha'\nu'}(q'); \quad \alpha\nu = c0, s1, c1. \quad (3)$$

On the right-hand side of this equation $\Delta N_{\alpha\nu}(q) = \Delta \mathcal{N}_{\alpha\nu}(\bar{q})$ is the bare-momentum distribution function deviation $\Delta N_{\alpha\nu}(q) = N_{\alpha\nu}(q) - N_{\alpha\nu}^0(q)$ [18] and the elementary two-pseudofermion phase shifts $\Phi_{\alpha\nu, \alpha'\nu'}(q, q')$ in units of π are defined in Eqs. (15) and (A1)-(A13) of Ref. [17]. According to the pseudofermion scattering theory of Refs. [20, 21], $+\pi \Phi_{\alpha\nu, \alpha'\nu'}(q, q')$ (and $-\pi \Phi_{\alpha\nu, \alpha'\nu'}(q, q')$) gives the phase shift acquired by the bare-momentum q $\alpha\nu$ pseudofermion or hole wave function when such an object is scattered by a bare-momentum q' $\alpha'\nu'$ pseudofermion (and $\alpha'\nu'$ pseudofermion hole) created under a ground-state - excited-energy-eigenstate transition. The bare-momentum distribution-function deviations $\Delta N_{\alpha'\nu'}(q')$ of Eq. (3) result from such a transition. In expression (3) it is assumed that these deviations describe excited energy eigenstates generated by one-electron dominant processes. The corresponding general expression is given in Eq. (14) of Ref. [17] and involves summations over all pseudofermion branches.

Note that for each $\alpha\nu$ branch the continuum bare-momentum q corresponds to a set of discrete bare momentum values q_j such that $q_{j+1} - q_j = 2\pi/L$. Here $j = 1, 2, \dots, N_{\alpha\nu}^*$ and the number $N_{\alpha\nu}^* = N_{\alpha\nu} + N_{\alpha\nu}^h$ is given in Eqs. (B6)-(B8) and (B11) of Ref. [15]. $N_{\alpha\nu}$ and $N_{\alpha\nu}^h$ denote the number of $\alpha\nu$ pseudofermions and $\alpha\nu$ pseudofermion holes, respectively. $N_{\alpha\nu}^*$ equals the number of sites of the effective $\alpha\nu$ lattice [17], which plays an important role in the pseudoparticle and pseudofermion descriptions. For the PS where the finite-number-electron excitations are contained, the number $N_{\alpha\nu}^*$ can for $\nu > 0$ be written as,

$$N_{\alpha\nu}^* = N_{\alpha\nu}^{0,*} + \Delta L_{\alpha} + 2 \sum_{\nu'=\nu+1}^{\infty} (\nu' - \nu) N_{\alpha\nu'}; \quad \alpha = c, s, \quad \nu > 0. \quad (4)$$

Here

$$N_{c\nu}^{0,*} = (N_a - N); \quad N_{s1}^{0,*} = N_{\uparrow}; \quad N_{s\nu}^{0,*} = (N_{\uparrow} - N_{\downarrow}), \quad \nu > 1, \quad (5)$$

are the ground-state values for that number, $N_{\alpha\nu}$ is the number of $\alpha\nu$ pseudofermions (and pseudoparticles), and ΔL_{α} is the deviation from the ground-state value of the number L_{α} of Yang holons ($\alpha = c$) or HL spinons ($\alpha = s$)

defined in Eq. (33) of Ref. [15]. On the other hand, $N_{c0}^{0,*} = N_{c0}^*$ is given by $N_{c0}^* = N_a$ for the whole Hilbert space. Expressions (4) and (5) refer to all the infinite $\alpha\nu$ pseudofermion branches but also apply to our case where only the $\alpha\nu = c0, s1, c1$ branches have finite pseudofermion occupancy in the excited energy eigenstates.

Although the $\alpha\nu$ pseudoparticles carry bare-momentum q [15, 16, 17], one can also label the corresponding $\alpha\nu$ pseudofermions by that bare-momentum. Indeed, the latter pseudofermions carry canonical-momentum $\bar{q} = q + Q_{\alpha\nu}^\Phi(q)/L$, but this latter expression provides an one-to-one relation between the bare-momentum q and the canonical-momentum \bar{q} . The pseudoparticles have residual-interaction energy terms which do not allow the excited-state wave function to factorize into $\alpha\nu$ pseudoparticle wave functions [17]. A property which plays a central role in the PDT is that for the corresponding $\alpha\nu$ pseudofermions, such a residual-interaction energy terms are exactly canceled by the scattering phase shift $Q_{\alpha\nu}^\Phi(q)/2$. By canceling the residual interactions exactly, the associated canonical-momentum shift $Q_{\alpha\nu}^\Phi(q)/L$ transfers the information recorded in these interactions over to the pseudofermion canonical momentum. It is shown in Refs. [20, 21] that the $\alpha\nu$ pseudofermion or $\alpha\nu$ pseudofermion hole overall phase shift acquired under a ground-state - excited-energy-eigenstate transition is given by $Q_{\alpha\nu}(q)/2 = Q_{\alpha\nu}^0/2 + Q_{\alpha\nu}^\Phi(q)/2$. Here $Q_{\alpha\nu}^\Phi(q)/2$ is given in Eq. (3) and $Q_{\alpha\nu}^0/2 = 0, \pm\pi/2$ in Eq. (11) of Ref. [17]. $Q_{\alpha\nu}^0/2$ is a $\alpha\nu$ pseudoparticle or hole overall scattering-less phase shift. It is such that under a ground-state - excited-energy-eigenstate transition the $\alpha\nu$ pseudoparticle and hole discrete bare-momentum value q_j is shifted by $Q_{\alpha\nu}^0(q_j)/L$. The overall phase shift $Q_{\alpha\nu}(q)/2$ leads to a corresponding canonical-momentum shift $Q_{\alpha\nu}(q_j)/L$ for the discrete canonical-momentum values of the $\alpha\nu$ pseudofermions and holes. According to the studies of Refs. [20, 21], the overall phase shift $Q_{\alpha\nu}(q)/2$ is associated with the $\alpha\nu$ pseudofermion or hole S matrix $\exp\{iQ_{\alpha\nu}(q)\}$.

The pseudofermions have energy bands $\epsilon_{c0}(q)$, $\epsilon_{s1}(q)$, and $\epsilon_{c1}(q) = E_u + \epsilon_{c1}^0(q)$ such that $|q| \leq \pi$, $|q| \leq k_F$, and $|q| \leq [\pi - 2k_F]$, respectively. These energy dispersions are plotted in Figs. 6-9 of Ref. [16]. The energy bands are defined in Eqs. (C.15)-(C.21) of Ref. [15] and the correlation energy parameter $E_u = 2\mu$ is defined in Ref. [19]. Also the group velocity $v_{\alpha\nu}(q) = \partial\epsilon_{\alpha\nu}(q)/\partial q$ and the *light* velocity $v_{\alpha\nu} \equiv v_{\alpha\nu}(q_{F\alpha\nu}^0)$ for $\alpha\nu = c0$ and $\alpha\nu = s1$ appear in the spectral-function expressions. In Sec. III we confirm that the pseudofermion energy bands fully determine the shape of the one-electron spectral-function in the proximity of the branch lines studied in that section. The correlation energy parameter E_u defines the lower-limit of the *upper-Hubbard band* (UHB) [18]. The creation onto the ground state of $c1$ pseudofermions or $-1/2$ Yang holons is always a finite-energy process. Indeed, $\omega = E_u$ and $k = \pi$ are the energy and momentum, respectively, for creation onto the ground state of a dispersion-less $-1/2$ Yang holon. Similarly, E_u is the minimum energy value for the creation onto the ground state of a $c1$ pseudofermion. The correlation energy parameter E_u is an increasing function of U and a decreasing function of the density n with the following limiting values,

$$E_u = 4t \cos(\pi n/2), \quad U/t \rightarrow 0; \quad U + 4t \cos(\pi n), \quad U/t \rightarrow \infty; \quad U + 4t, \quad n \rightarrow 0; \quad E_{MH}, \quad n \rightarrow 1, \quad (6)$$

where E_{MH} is the half-filling Mott-Hubbard gap [5]. In the ground state there are no $-1/2$ Yang holons, the $c1$ and $s1$ pseudofermion bands are empty and filled, respectively, and the $c0$ pseudofermions occupy the bare-momentum domain $0 \leq |q| \leq 2k_F$ (leaving $2k_F < |q| \leq \pi$ empty).

The initial ground state and excited energy eigenstates of Eq. (2) that are associated with the one-electron dominant processes can be expressed in terms of occupancy configurations of the above quantum objects. The first step of the evaluation of the spectral functions (2) involves the expression of the electronic operators in terms of these quantum objects, as described in Refs. [18, 19]. For one-electron removal, the dominant processes involve creation of one pseudofermion hole both in the bands $\epsilon_{c0}(q)$ and $\epsilon_{s1}(q)$. For one-electron addition, these dominant processes lead to two spectral features: A *lower-Hubbard band* (LHB) generated by creation of one pseudofermion in $\epsilon_{c0}(q)$ and one pseudofermion hole in $\epsilon_{s1}(q)$; A UHB generated by creation of one pseudofermion hole both in $\epsilon_{c0}(q)$ and $\epsilon_{s1}(q)$ and one pseudofermion in $\epsilon_{c1}^0(q)$ (or one $-1/2$ Yang holon for $n = 1$). The excited energy eigenstates generated by these one-electron dominant processes belong to subspaces whose $c0$ pseudofermion, $s1$ pseudofermion hole, $c1$ pseudofermion, and $-1/2$ Yang holon number ground-state deviations are given by,

$$\Delta N_{c0} = 1, \quad \Delta N_{s1}^h = 1, \quad \Delta N_{c1} = \Delta L_{c,-1/2} = 0; \quad 0 < n < 1, \quad (7)$$

for LHB one-electron addition,

$$\Delta N_{c0} = -1, \quad \Delta N_{s1}^h = 1, \quad \Delta N_{c1} = 1, \quad \Delta L_{c,-1/2} = 0; \quad 0 < n < 1, \quad (8)$$

and

$$\Delta N_{c0} = -1, \quad \Delta N_{s1}^h = 1, \quad \Delta N_{c1} = 0, \quad \Delta L_{c,-1/2} = 1; \quad n = 1, \quad (9)$$

for UHB one-electron addition, and

$$\Delta N_{c0} = -1, \quad \Delta N_{s1}^h = 1, \quad \Delta N_{c1} = \Delta L_{c,-1/2} = 0, \quad (10)$$

for one-electron removal. Moreover, we find in Sec. III that most one-electron spectral-function singular features are associated with the charge $c0$ or spin $s1$ pseudofermion branch lines. Since for $m \rightarrow 0$ the $s1$ band is full for the initial ground state, the one-electron spectral-function singular $s1$ branch lines are always associated with creation of one hole in the $s1$ pseudofermion band, as confirmed by Eqs. (7)-(10). Note that while $N_{c0}^h = N_a - N_{c0}$, the general expression for the number of $\alpha\nu = s1$ pseudofermion holes provided in Eqs. (B7) and (B11) of Ref. [15] can be simplified to,

$$N_{s1}^h = N_{c0} - 2 \sum_{\nu'=1}^{\infty} N_{s\nu'}, \quad (11)$$

where $N_{s1}^h = N_{c0} - 2N_{s1} = 0$ for the initial ground state and $N_{s1}^h = N_{c0} - 2N_{s1} = 1$ for the excited energy eigenstates associated with the deviations (7)-(10).

For half-filling there is no LHB and the UHB processes associated with the deviations given in Eq. (8) are not allowed. In contrast, for finite values of the doping concentration $\delta = [1 - n] > 0$ only the processes associated with the deviations of Eq. (8) lead to finite contributions to the UHB one-electron spectral-weight distribution [18]. As mentioned above, use of the PDT reveals that as we approach the pseudofermion branch lines in the (k, ω) -plane, only the excited energy eigenstates belonging to the subspaces associated with the dominant one-electron processes contribute to the spectral weight.

The domains of the (k, ω) -plane whose spectral weight is generated by one-electron dominant processes are shown in Fig. 1, where one-electron removal, LHB addition, and UHB addition corresponds to $\omega < 0$, $0 < \omega < E_u$, and $\omega > E_u$, respectively. The dominant processes also include pseudofermion particle-hole processes that lead to spectral weight both inside and outside but in the close vicinity of the shaded domains of Fig. 1. The figure corresponds to the extended momentum scheme used in this paper.

II. THE PSEUDOFERMION BRANCH-LINE GENERAL EXPRESSIONS AND ASSOCIATED QUANTITIES

The general finite-number-electron spectral function expressions obtained in Refs. [18, 19] by means of the PDT can be evaluated for the whole (k, ω) -plane with the help of suitable numerical calculations. In this paper we present an application to the study of the one-electron spectral-weight distribution in the vicinity of the branch lines introduced in that reference. Most of the singular features and spectral-weight edges are located on these lines. They are generated by processes where a specific $\alpha\nu$ pseudofermion or $\alpha\nu$ pseudofermion hole is created for all the available values of bare-momentum q and the remaining quantum objects are created at their *Fermi points* $\pm q_{F\alpha'\nu'}^0$ for the $\alpha'\nu' = c0, s1$ branches and at the limiting bare-momentum values $\pm q_{c1}^0 = \pm[\pi - 2k_F]$ for the $c1$ branches. The detailed derivation of the general spectral-function expressions in the vicinity of such lines is presented in Ref. [19].

A. THE GENERAL EXPRESSIONS FOR THE PSEUDOFERMION BRANCH LINES

According to the results of Ref. [19], for densities $0 < n < 1$ and $0 < m < n$ the functional,

$$2\Delta_{\alpha\nu}^{\iota} = \left(\iota \Delta N_{\alpha\nu, \iota}^{0,F} + \frac{Q_{\alpha\nu}(\iota q_{F\alpha\nu}^0)}{2\pi} \right)^2 = \left(\iota \Delta N_{\alpha\nu, \iota}^F + \frac{Q_{\alpha\nu}^{\Phi}(\iota q_{F\alpha\nu}^0)}{2\pi} \right)^2; \quad \iota = \pm 1; \quad \alpha\nu = c0, s1, \quad (12)$$

controls the expressions of the spectral-function branch-line exponents. Here $\Delta N_{\alpha\nu, \iota}^F$ is the deviation in the number of $\alpha\nu = c0, s1$ pseudofermions at the *Fermi points* and $Q^{\Phi}(\iota q_{F\alpha\nu}^0)/2$ and $Q_{\alpha\nu}(\iota q_{F\alpha\nu}^0)/2 = Q_{\alpha\nu}^0/2 + Q^{\Phi}(\iota q_{F\alpha\nu}^0)/2$ are the overall scattering and overall, respectively, phase shifts of $\alpha\nu$ pseudofermion or hole scatterers at the bare-momentum *Fermi values* $\iota q_{F\alpha\nu}^0 = \pm q_{F\alpha\nu}^0$. Note that the deviation $\Delta N_{\alpha\nu, \iota}^F = \iota \Delta N_{\alpha\nu, \iota}^{0,F} + Q_{\alpha\nu}^0/2\pi$ involves both contributions from the overall scattering-less phase shift $Q_{\alpha\nu}^0/2$ and the number deviation $\Delta N_{\alpha\nu, \iota}^{0,F}$ generated by the creation or annihilation pseudofermion processes at the *Fermi points*. We also consider the $\alpha\nu = c0, s1$ current number deviation $2\Delta J_{\alpha\nu}^F = \Delta N_{\alpha\nu, +1}^F - \Delta N_{\alpha\nu, -1}^F$ and the current number $2J_{c1}^F = N_{c1, +1}^F - N_{c1, -1}^F$, where $N_{c1, \iota}^F$

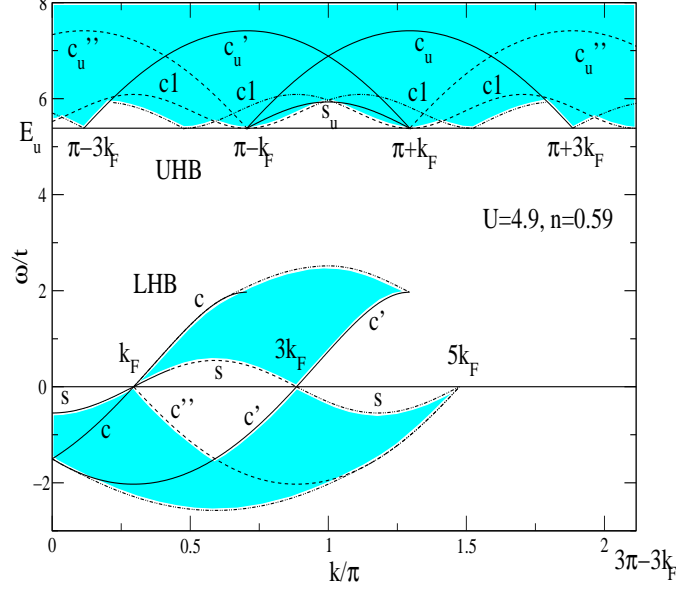


FIG. 1: Extended-zone scheme centered at $k = 0$ (and at $k = \pi$ for the UHB) for $U = 4.9t$ and $n = 0.59$. (These are the U/t and n values found in Sec. V for the spectral features associated with the TCNQ stacks.) The shaded areas weight is generated by one-electron dominant processes. The energy E_u defines the lower limit of the UHB. The solid and dashed lines denoted by the letters $c, c', c'', s, c_u, c'_u, c''_u$, and c_l are singular and edge branch lines, respectively. The momentum and energy dependence of the weight distribution in the vicinity of such branch lines is studied in Sec. III.

with $\iota = \pm 1$ is the number of c_l pseudofermions created at the limiting bare-momentum $q = \iota[\pi - 2k_F]$ such that $\iota = \pm 1$. In turn, $N_{c_l}^{NF}$ denotes the number of c_l pseudofermions created at bare-momentum values $|q| < [\pi - 2k_F]$. For the UHB considered below these numbers can have the following values: $\{N_{c_l, +1}^F = 1, N_{c_l, -1}^F = 0, N_{c_l}^{NF} = 0\}$, $\{N_{c_l, +1}^F = 0, N_{c_l, -1}^F = 1, N_{c_l}^{NF} = 0\}$, and $\{N_{c_l, +1}^F = 0, N_{c_l, -1}^F = 0, N_{c_l}^{NF} = 1\}$.

Here and in sections III and IV we label the $\alpha\nu$ pseudofermions by their bare-momentum q , which is related to the canonical momentum as $\bar{q} = q + Q_{\alpha\nu}^\Phi(q)/L$. The momentum values k of the $\alpha\nu$ branch lines points $(k, l\omega_{\alpha\nu}(k))$ are determined by the bare-momentum value q of the created $\alpha\nu$ pseudofermion or hole by the following parametric equations,

$$\begin{aligned} k &= l \left[k_0 + c_1 c_{\alpha\nu} q \right]; & q &= c_1 c_{\alpha\nu} \left[l k - k_0 \right]; & \omega_{\alpha\nu} &= c_1 \epsilon_{\alpha\nu}(q); \\ k_0 &= 4k_F \left[\Delta J_{c_0}^F + J_{c_l}^F \right] + 2k_{F\downarrow} \Delta J_{s_1}^F - 2\pi J_{c_l}^F. \end{aligned} \quad (13)$$

Here the index $l = \pm 1$ is that of the corresponding spectral function $B^l(k, \omega)$ of Eq. (2) and the constants c_1 and $c_{\alpha\nu}$ are such that $c_1 = +1$ (and $c_1 = -1$) for creation of a $\alpha\nu$ pseudofermion (and a $\alpha\nu$ pseudofermion hole) and $c_{\alpha\nu} = 1$ for $\alpha\nu = c_0, s_1$ and $c_{c_l} = -1$, respectively. The spectral-function expressions studied below also involve the group velocity $v_{\alpha\nu}(q) = \partial \epsilon_{\alpha\nu}(q) / \partial q$ for the $\alpha\nu = c_0, s_1, c_l$ branches and the *Fermi point* velocity $v_{\alpha\nu} \equiv v_{\alpha\nu}(q_{F\alpha\nu}^0)$ for the $\alpha\nu = c_0, s_1$ branches.

According to the studies of Ref. [19], the one-electron spectral functions (2) have in the vicinity of the $\alpha\nu$ branch lines the following power-law expression for values of energy ω such that $l(\omega - l\omega_{\alpha\nu}(q))$ is small and positive where the point $(k, l\omega_{\alpha\nu}(q))$ belongs to the branch line,

$$\begin{aligned}
B^l(k, \omega) &\approx C_{\alpha\nu}(q) \left(\frac{l[\omega - l\omega_{\alpha\nu}(q)]}{4\pi\sqrt{v_{c0}v_{s1}}} \right)^{\zeta_{\alpha\nu}(q)}; \quad \zeta_{\alpha\nu}(q) > -1 \\
&= \delta(\omega - l\omega_{\alpha\nu}(q)); \quad \zeta_{\alpha\nu}(q) = -1; \quad \alpha\nu = c0, s1, c1.
\end{aligned} \tag{14}$$

Here $q = c_1 c_{\alpha\nu} [lk - k_0]$, the first expression is the leading-order term of a power-law expansion in the small energy deviation $l[\omega - l\omega_{\alpha\nu}(k)]$ relative to the branch-line energy, and the exponent $\zeta_{\alpha\nu}(k)$ and the function $C_{\alpha\nu}(k)$ have the following general form,

$$\begin{aligned}
\zeta_{\alpha\nu}(q) &= -1 + \zeta_0(q); \quad \zeta_0(q) = 2\Delta_{c0}^{+1}(q) + 2\Delta_{c0}^{-1}(q) + 2\Delta_{s1}^{+1}(q) + 2\Delta_{s1}^{-1}(q) \geq 0; \\
C_{\alpha\nu}(q) &= \frac{\text{sgn}(q) c_{\alpha\nu}}{2\pi n_{\alpha\nu}^*} \int_{-\frac{\text{sgn}(q) c_{\alpha\nu}}{v_{s1}}}^{\frac{1}{2v_{\alpha\nu}(q) + \text{sgn}(q) c_{\alpha\nu} v_{s1}}} dz \frac{F_0(z)}{[1 - z v_{\alpha\nu}(q)]^{\zeta_0(q)}} \geq 0,
\end{aligned} \tag{15}$$

where $n_{\alpha\nu}^* = N_{\alpha\nu}^*/L$, $F_0(z)$ is an even function of z which is defined in Ref. [19], and the functional $2\Delta_{\alpha\nu}^\iota$ is given in Eq. (12). Although such a functional refers to the $c0$ and $s1$ pseudofermions only, note that the scattering phase-shift (3), which is part of the expression (12), *feels* the bare-momentum distribution-function deviations of all the $\alpha\nu$ pseudofermion branches with finite occupancy in the excited energy eigenstate. A quantitative study of the function $C_{\alpha\nu}(q)$ whose general expression is provided in Eq. (15) involves the numerical derivation of the lowest-peak weight functional introduced in Ref. [19], which is included in the expression of the function $F_0(z)$. Such a quantitative study is beyond the goals of this paper and will be carried out elsewhere. However, the general $C_{\alpha\nu}(q)$ expression of Eq. (15) is useful for our studies, once it provides information about the behavior of the function $C_{\alpha\nu}(q)$ as $U/t \rightarrow 0$ and can be used to find out whether for finite values of U/t that function is vanishing or finite and also what its relative value for different branch lines is.

A $\alpha\nu$ branch line whose exponent $\zeta_{\alpha\nu}(q)$ is negative for a given domain of $k = l[k_0 + c_1 c_{\alpha\nu} q]$ values is called a singular branch line. In this case the weight distribution shows a singular behavior at the branch line, and we expect that the spectral peaks will be observed in a real experiment. This is confirmed for one-electron removal in Sec. V. On the other hand, when for a given k domain the exponent (15) is such that $0 < \zeta_{\alpha\nu}(q) < 1$ the corresponding line refers to an edge branch line. Finally, $\zeta_{\alpha\nu}(q) > 1$ for a k domain is in general a sign of near absence of spectral weight. The concept of pseudofermion branch line refers to the domains of momentum k where the exponent (15) is such that $\zeta_{\alpha\nu}(q) < 1$. The singular and edge branch lines are represented in Fig. 1 by solid and dashed lines, respectively. The dashed-dotted lines of that figure are either border lines for the domains of weight generated by dominant processes or lines associated with exponents larger than one. The latter lines have very little weight. However, for finite values of U/t some of the former border lines correspond to singular spectral features, as discussed in Sec. IV.

We note that for the $\alpha\nu = c0, s1$ branches the general branch-line spectral-function expressions defined by Eqs. (14) and (15) are not valid in the vicinity of the branch-line end points. Such end points correspond to values of k and ω such that $\omega \approx \iota v_{\alpha\nu}(k - lk_0) + l E_u N_{c1}$, where $\alpha\nu = c0, s1$ and $\iota = \pm 1$. When these points correspond to vanishing energy such that $N_{c1} = 0$, the physics is that of the so called low-energy Tomanaga-Luttinger liquid (TLL) regime, where bosonization [8] and conformal-field theory [9] are applicable.

B. LIMITING BEHAVIOR NEAR THE BRANCH-LINE END POINTS

For values of k and ω such that $\omega \approx \iota v_{\alpha\nu}(k - lk_0) + l E_u N_{c1}$, where $\alpha\nu = c0, s1$ and $\iota = \pm 1$, the general PDT leads to the following spectral function expression,

$$\begin{aligned}
B^l(k, \omega) &\approx C_{\alpha\nu, \iota} \left(\frac{l[\omega - l(E_u N_{c1} + \iota v_{\alpha\nu}(k - lk_0))]}{4\pi\sqrt{v_{c0}v_{s1}}} \right)^{-1 + \zeta_{\alpha\nu, \iota}^0}; \quad \zeta_{\alpha\nu, \iota}^0 = \zeta_{\alpha\nu}^0 - 2\Delta_{\alpha\nu}^{-\iota} \geq 0; \\
C_{\alpha\nu, \iota} &= \frac{\iota}{2\pi n_{\alpha\nu}^*} \int_{-\frac{\iota}{v_{\alpha\nu}}}^{\frac{\iota}{2v_{\alpha\nu} + v_{\alpha\nu}}} dz \frac{F_{\alpha\nu, \iota}^0(z)}{(1 - \iota z v_{\alpha\nu})^{\zeta_{\alpha\nu, \iota}^0}} \geq 0; \quad \alpha\nu = c0, s1; \quad \iota = \pm 1,
\end{aligned} \tag{16}$$

where $F_{\alpha\nu, \iota}^0(z)$ is an even function of z [19]. The spectral function expression given in Eq. (16) refers to the proximity of a $\alpha\nu = c0, s1$ branch-line end point and differs from the corresponding general spectral function expression provided in Eq. (14). The latter expression applies in the vicinity of the $\alpha\nu = c0, s1$ branch lines when the $\alpha\nu = c0, s1$ branch-line group velocity $v_{\alpha\nu}(q)$ is such that $v_{\alpha\nu}(q) \neq \iota v_{\alpha\nu}$. As the value of $v_{\alpha\nu}(q)$ approaches that of the *Fermi point*

velocities $\pm v_{\alpha\nu}$, $v_{\alpha\nu}(q) \rightarrow \iota v_{\alpha\nu}$, the spectral function k and ω values reach the vicinity of a branch-line end point and thus the spectral function is given by expression given in Eq. (16) instead of that defined by Eqs. (14) and (15).

Interestingly, for $\omega \approx \iota v_{\alpha\nu}(k - lk_0)$ and thus $N_{c1} = 0$ the validity of the spectral-function expression given in Eq. (16) corresponds to the TLL regime. Therefore, in this limit the above exponent $-1 + \zeta_{\alpha\nu, \iota}^0$ provided by the general PDT of Ref. [18] must equal that obtained by the use of the low-energy bosonization [8], conformal-field theory [9], and other techniques. Indeed, it is straightforward to show that the general exponent (16) is that given in Eq. (5.7) of Ref. [9]. We emphasize that the k domain corresponding to the TLL exponent (16) has an infinitesimal width and corresponds to the limit when the $\alpha\nu = c0$ or $\alpha\nu = s1$ branch-line group velocity is such that $v_{\alpha\nu}(q) \approx \pm v_{\alpha\nu}$. There is a small cross-over region between the two regimes. As further discussed in Sec. V, in the latter small low-energy region the 1D Hubbard model does not apply to the description of the spectral properties of TTF-TCNQ: In addition to correlation effects, at low energy such spectral properties involve inter-chain hopping and electron-phonon interactions.

In this paper we do not consider the limiting case associated with the expression (16). While that expression is valid along a branch-line domain of infinitesimal measure, the spectral-function expression associated with the general exponent (15) refers to the vicinity of the whole branch line, except for specific branch-line points mentioned above and for a small cross-over region between the two regimes. The momentum width of the latter region is small and vanishes as $U/t \rightarrow 0$. In this limit the general branch-line spectral-function expressions defined by Eqs. (14) and (15) lead to the correct $U/t = 0$ spectral-weight distributions, as confirmed below in Sec. IV. Thus, for branch lines with end points at vanishing energy the TLL spectral-function expression (16) is valid in a domain of infinitesimal measure. In contrast, the general exponent (15) cannot be obtained by the above-mentioned TLL low-energy methods and is valid in the vicinity of nearly the whole branch line.

From the use of conformal-field theory [28], it is known that when the above branch-line end points $(k_0, 0)$ are reached through low-energy lines other than the above branch lines the spectral-function expression is different and controlled by another exponent. According to the PDT of Refs. [18, 19], the same occurs for all above branch-line end points $(lk_0, l\omega_0)$ such that $\omega_{\alpha\nu} \equiv \omega_0 = E_u N_{c1}$. Examples of such points are $(k = \pm k_F, \omega = 0)$, $(k = \pm 3k_F, \omega = 0)$, $(k = \pi \pm k_F, \omega = E_u)$, and $(k = \pi \pm 3k_F, \omega = E_u)$. (These points are represented in Fig. 1 for $k > 0$, where for the one-electron dominant processes $\omega_0 = 0, E_u$.) The general theory provides spectral-function expressions that are valid when these points are approached by lines that are contained in the finite-weight regions and do not cross the $\alpha\nu$ branch lines ending at the same points. Indeed, following the studies of Ref. [19], in the proximity of the $(lk_0, l\omega_0)$ point but for values of k and ω such that $\omega \approx v(k - lk_0) + l\omega_0$ where $-v_{s1} < v < v_{s1}$ and $v \neq \pm v_{s1}, \pm v_{c0}$ the momentum and energy weight-distribution dependence has the following general expression,

$$\begin{aligned} B^l(k, \omega) &\approx \frac{C_0(v)}{4\pi \sqrt{v_{c0} v_{s1}}} \left(\frac{l[\omega - l\omega_0]}{4\pi \sqrt{v_{c0} v_{s1}}} \right)^{-2+\zeta_0}; \quad -2 + \zeta_0 > -1, \\ &= \delta(\omega - l\omega_0) \delta_{k, lk_0}; \quad -2 + \zeta_0 = -1, \end{aligned} \quad (17)$$

where the function $C_0(v)$ is such that $C_0(v) = F_0(1/v)$ where $F_0(z)$ is the function appearing in Eq. (15), which is defined in Ref. [19], and ζ_0 is the above functional $\zeta_0 = 2\Delta_{c0}^{+1} + 2\Delta_{c0}^{-1} + 2\Delta_{s1}^{+1} + 2\Delta_{s1}^{-1}$. Here $2\Delta_{\alpha\nu}^{\iota}$ is the functional of Eq. (12) for the bare-momentum distribution function deviations associated with the excitations that control the spectral-weight distribution in the vicinity of the point $(k = lk_0, \omega = l\omega_0)$. Moreover, the velocity $v = (\omega - l\omega_0)/(k - lk_0) \neq \pm v_{c0}$ such that $|v| < v_{s1}$ plays an important role in the spectral properties [19]. We note that for $\omega_0 = 0$ and $k = lk_0$ the ω dependence of the spectral-function (17) is that obtained by conformal-field theory in Ref. [28]. Expression (17) can be derived by other methods [27]. Since the power-law spectral-function expression (17) was already studied in Ref. [27] and refers to the vicinity of isolated points in the (k, ω) -plane, here we limit our study to the more complex problem of the branch-line spectral weight.

For excited energy eigenstates generated by processes involving pseudofermion occupancies in the vicinity of the $c0$ or $s1$ *Fermi points*, the functional (12) and the corresponding branch-line exponent expressions of Sec. III involve the following elementary two-pseudofermion phase shift parameters,

$$\xi_{\alpha\nu\alpha'\nu'}^j = \delta_{\alpha,\alpha'} \delta_{\nu,\nu'} + \sum_{\iota=\pm 1} (\iota^j) \Phi_{\alpha\nu,\alpha'\nu'}(q_{F\alpha\nu}^0, \iota q_{F\alpha'\nu'}^0); \quad j = 0, 1; \quad \alpha\nu = c0, s1; \quad \alpha'\nu' = c0, s1. \quad (18)$$

In the limit $m \rightarrow 0$, these parameters are given by $\xi_{c0c0}^0 = 1/\xi_0$, $\xi_{c0s1}^0 = 0$, $\xi_{s1c0}^0 = -1/\sqrt{2}$, $\xi_{s1s1}^0 = \sqrt{2}$, $\xi_{c0c0}^1 = \xi_0$, $\xi_{c0s1}^1 = \xi_0/2$, $\xi_{s1c0}^1 = 0$, and $\xi_{s1s1}^1 = 1/\sqrt{2}$. Here ξ_0 is the parameter defined in Eq. (74) of Ref. [26] and in the text above that equation. It is such that $\xi_0 \rightarrow \sqrt{2}$ and $\xi_0 \rightarrow 1$ as $U/t \rightarrow 0$ and $U/t \rightarrow \infty$, respectively. For $U/t \gg 1$ the

t/U expansion of that parameter is up to first order given by,

$$\xi_0 = 1 + \frac{4t}{\pi U} \ln 2 \sin(\pi n); \quad U/t \gg 1. \quad (19)$$

III. THE ONE-ELECTRON BRANCH LINES

In this section we use the general branch-line expressions and associated quantities considered above in the study of the one-electron spectral-function singular and edge branch lines.

A. THE ONE-ELECTRON REMOVAL BRANCH LINES

The ground-state - excited-energy-eigenstate transitions to the subspace whose pseudofermion number deviations are given in Eq. (10), generate several $\alpha\nu$ pseudofermion branch lines whose location in the (k, ω) -plane is shown in the Fig. 1 for $\omega < 0$. The $s \equiv s1$ branch-line shown in the figure, which connects the points $(k = -k_F, \omega = 0)$ and $(k = k_F, \omega = 0)$, is generated by creating the $c0$ pseudofermion hole at one of its pseudo-Fermi points, and creating the $s1$ pseudofermion hole for bare-momentum values in the domain defined by the inequality $|q| \leq k_F$. This line is labeled by s in Fig. 1, where it is represented for positive values of momentum such that $0 < k < k_F$ and $\omega \leq 0$. We emphasize that in addition to creation of a $c0$ pseudofermion hole at $q = 2k_F$ (and $q = -2k_F$), this excitation includes a collective bare-momentum shift $Q_{c0}^0/L = +\pi/L$ (and $Q_{c0}^0/L = -\pi/L$) for the whole $c0$ pseudofermion *Fermi sea*. The associated scattering-less pseudoparticle phase shift $Q_{c0}^0/2$ is defined in Eq. (11) of Ref. [17].

By considering the same processes, plus transferring a $c0$ pseudofermion from the *Fermi point* $-\iota' 2k_F$ to the *Fermi point* $\iota' 2k_F$, two other $s1$ branch lines are generated, which connect the points $(k = -\iota' 3k_F, \omega = 0)$ and $(k = -\iota' 5k_F, \omega = 0)$ where $\iota' = \pm 1$. The $\iota' = -1$ line is labeled by s in Fig. 1, where it appears for $\omega \leq 0$. On the other hand, there are four $c0$ pseudofermion branches lines which connect the points $(k = -3k_F, \omega = 0)$ and $(k = k_F, \omega = 0)$, $(k = -k_F, \omega = 0)$ and $(k = 3k_F, \omega = 0)$, $(k = -5k_F, \omega = 0)$ and $(k = -k_F, \omega = 0)$, and $(k = k_F, \omega = 0)$ and $(k = 5k_F, \omega = 0)$. The first, second, and fourth of these lines are labeled by c , c' , and c'' , respectively, in Fig. 1, where their $k > 0$ parts are shown for $\omega \leq 0$. Below we study the spectral-weight distribution in the vicinity of these seven one-electron removal branch lines.

We start by evaluating the weight distribution corresponding to the first $s1$ pseudofermion branch line mentioned above. The specific form of the general expressions (13) for the points $(k, -\omega_{s1}(k))$ belonging to the $s1$ pseudofermion branch line in the $m \rightarrow 0$ limit, corresponds to $k_0 = 0$ and $l = c_1 = -c_{s1} = -1$ and reads,

$$q = k; \quad -\omega_{s1}(q) = \epsilon_{s1}(q). \quad (20)$$

Here, $\epsilon_{s1}(q)$ is the energy dispersion given in Eq. (C.16) of Ref. [15] and plotted for $m \rightarrow 0$ in Fig. 7 of Ref. [16]. (The energy dispersions $\epsilon_{c0}(q)$, $\epsilon_{s1}(q)$, and $\epsilon_{c1}^0(q)$ such that $\epsilon_{c1}(q) = E_u = \epsilon_{c1}^0(q)$ appearing in other expressions of this subsection are those defined in Eqs. (C.15)-(C.17) of Ref. [15] and plotted in Figs. 6-9 of Ref. [16].) We recall that the $k > 0$ part of this $s1$ pseudofermion singular branch line is labeled by s in Fig. 1, where it connects the points $(k = 0, \omega = \epsilon_{s1}(0))$ and $(k = k_F, \omega = 0)$. In this case the general spectral-function expression (14) applies provided that the specific expression associated with the excitations around the point $(k, -\omega_{s1}(k))$ of the functional $2\Delta_{\alpha\nu}^\iota$ defined in Eq. (12) is used. This expression is a function of $k = q$ and corresponds to the $m \rightarrow 0$ limit of the following quantity,

$$2\Delta_{\alpha\nu}^\iota(q) = \left\{ -\iota \frac{\xi_{\alpha\nu c0}^0}{2} - \Phi_{\alpha\nu, s1}(\iota q_{F\alpha\nu}, q) \right\}^2; \quad \alpha\nu = c0, s1. \quad (21)$$

Here the two-pseudofermion phase shift $\Phi_{\alpha\nu, s1}$ is defined by Eqs. (15), (A3), and (A7) of Ref. [17] for $\nu = 1$ and the parameter $\xi_{\alpha\nu c0}^0$ general expression is provided in Eq. (18). The two-pseudofermion phase shifts $\Phi_{\alpha\nu, \alpha'\nu'}$ appearing in other expressions of this subsection are those defined by Eqs. (15) and (A1)-(A13) of Ref. [17]. Moreover, the ground-state rapidity functions appearing in the arguments of the functions on the right-hand side of Eq. (13) of that reference are the inverse of the functions given in Ref. [19].

Direct use of the general expression (14) in the $m \rightarrow 0$ limit, leads to the following expression for the one-electron removal spectral function,

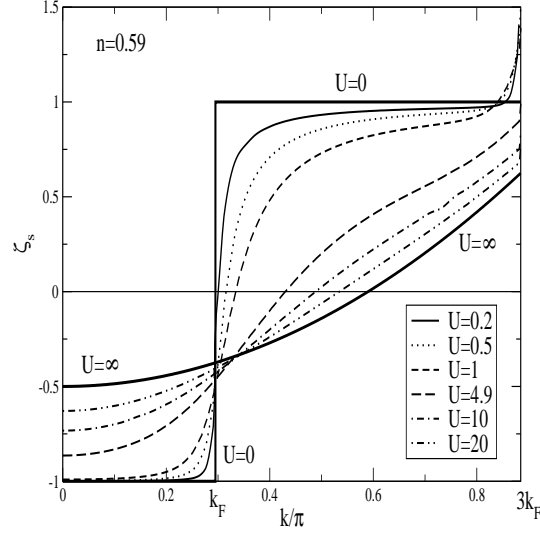


FIG. 2: Momentum dependence along the one-electron removal spin $s \equiv s1$ branch line of Fig. 1 for $0 < k < k_F$ and one-electron addition spin $s \equiv s1$, $+1$ branch line of the same figure for $k_F < k < 3k_F$ of the corresponding exponents (23) and (35), respectively. In the figure both these exponents are called ζ_s . We note that for very small momentum domains around $k = k_F$ and $k = 3k_F$, which correspond branch-line end points, this exponent does not apply, since the spectral function is of the form given in Eq. (16).

$$\begin{aligned}
 B^{-1}(k, \omega) &\approx C_{s1}(q) \left(\frac{-[\omega + \omega_{s1}(q)]}{4\pi\sqrt{v_{c0}v_{s1}}} \right)^{\zeta_{s1}(q)}; \quad \zeta_{s1}(q) > -1 \\
 &= \delta(\omega + \omega_{s1}(q)); \quad \zeta_{s1}(q) = -1,
 \end{aligned} \tag{22}$$

which corresponds to energy values just below the branch line and to bare-momentum and momentum values in the range $-k_F < q < k_F$ and $-k_F < k < k_F$, respectively. The function $C_{s1}(q)$ given in Eq. (15) is finite for all values of the q domain except at the branch line end points, where the spectral function is instead of the form given in Eq. (16). As the spin density m approaches zero, we find the following exponent expression valid for all values of U/t and electronic density n ,

$$\begin{aligned}
 \zeta_{s1}(q) &= -1 + \sum_{\alpha\nu=c0, s1} \sum_{\iota=\pm 1} \left\{ \frac{\xi_{\alpha\nu c0}^0}{2} + \iota \Phi_{\alpha\nu, s1}(\iota q_F^0, q) \right\}^2 \\
 &= -1 + \sum_{\iota=\pm 1} \left\{ \frac{1}{2\xi_0} + \iota \Phi_{c0, s1}(\iota 2k_F, q) \right\}^2 + \sum_{\iota=\pm 1} \left\{ -\frac{1}{2\sqrt{2}} + \iota \Phi_{s1, s1}(\iota k_F, q) \right\}^2,
 \end{aligned} \tag{23}$$

where the second expression was obtained by taking the limit $m \rightarrow 0$ in the first-expression quantities and the parameter ξ_0 is defined in Eq. (74) of Ref. [26]. The dependence of the exponent (23) on the momentum k is obtained by combining Eqs. (20) and (23). The exponent ζ_{s1} of Eq. (23) is negative for all values of momentum and is plotted in Fig. 2 as a function of the momentum k for $k > 0$, several values of U/t , and electronic density $n = 0.59$. So the corresponding spectral-function expression (22) describes a singular branch line. The exponent ζ_s of the figure is the exponent (23) for momentum values $0 < k < k_F$, whereas for $k_F < k < 3k_F$ ζ_s corresponds to a LHB one-electron addition exponent studied below. The $U/t \rightarrow 0$ and $U/t \rightarrow \infty$ limiting values of the exponent (23) and other exponents obtained in this section, are provided and discussed in the ensuing section.

Equivalent results are obtained for the other two one-electron removal $s1$ branch lines. We call them $s1, \iota'$ branch lines where $\iota' = \pm 1$. Here and in the expressions provided below we use the indices $\iota' = \pm 1$ and $\iota'' = \pm 1$ to denote contributions from processes which involve $c0$ and $s1$ pseudofermions, respectively, created or annihilated at the $m \rightarrow 0$ Fermi points $\iota' 2k_F = \pm 2k_F$ and $\iota'' k_F = \pm k_F$, respectively. For the $s1, \iota'$ branch lines, the index ι' refers to a $c0$ pseudofermion particle-hole process such that a $c0$ pseudofermion is annihilated at $q = -\iota' 2k_F$ and created at $q = \iota' 2k_F$, where $\iota' = \pm 1$. The specific form of the general expressions (13) for the points $(k, \omega_{s1, \iota'}(k))$ belonging to

the $s1, \iota'$ branch line in the $m \rightarrow 0$ limit, corresponds to $k_0 = \iota' 4k_F$ and $l = c_1 = -c_{s1} = -1$ and reads,

$$q = k + \iota' 4k_F; \quad \omega_{s1, \iota'}(q) = -\epsilon_{s1}(q). \quad (24)$$

The $s1, -1$ pseudofermion singular branch line is labeled by s in Fig. 1, where it connects the points $(k = 3k_F, \omega = 0)$ and $(k = 5k_F, \omega = 0)$. In this case the value of the functional (12) is a function of $k = q + \iota' 4k_F$ given by the $m \rightarrow 0$ limit of the parameter,

$$2\Delta_{\alpha\nu}^{\iota}(q) = \left\{ -\iota \frac{\xi_{\alpha\nu c0}^0}{2} + \iota' \xi_{\alpha\nu c0}^1 - \Phi_{\alpha\nu, s1}(\iota q_{F\alpha\nu}^0, q) \right\}^2; \quad \alpha\nu = c0, s1. \quad (25)$$

Use of the general expression (14) in the $m \rightarrow 0$ limit, leads to the following expression for the one-electron removal spectral function,

$$B^{-1}(k, \omega) \approx C_{s1, \iota'}(q) \left(\frac{-[\omega + \omega_{s1, \iota'}(q)]}{4\pi\sqrt{v_{c0} v_{s1}}} \right)^{\zeta_{s1, \iota'}(q)}. \quad (26)$$

This expression corresponds to energy values just below the branch line and to bare-momentum values in the range $-k_F < q < k_F$ and momentum values in the domains $-5k_F < k < -3k_F$ and $3k_F < k < 5k_F$ for $\iota' = 1$ and $\iota' = -1$, respectively. In the $m \rightarrow 0$ limit, we find the following exponent expression valid for all values of U/t and electronic density n ,

$$\begin{aligned} \zeta_{s, \iota'}(q) &= -1 + \sum_{\alpha\nu=c0, s1} \sum_{\iota=\pm 1} \left\{ \frac{\xi_{\alpha\nu c0}^0}{2} - \iota \iota' \xi_{\alpha\nu, c0}^1 + \iota \Phi_{\alpha\nu, s1}(\iota q_{F\alpha\nu}^0, q) \right\}^2 \\ &= -1 + \sum_{\iota=\pm 1} \left\{ \frac{1}{2\xi_0} - \iota \iota' \xi_0 + \iota \Phi_{c0, s1}(\iota 2k_F, q) \right\}^2 + \sum_{\iota=\pm 1} \left\{ -\frac{1}{2\sqrt{2}} + \iota \Phi_{s1, s1}(\iota k_F, q) \right\}^2. \end{aligned} \quad (27)$$

The dependence of the exponent (27) on the momentum k is obtained by combining Eqs. (24) and (27). For most of the parameter space and bare-momentum values, this exponent is larger than one and thus the spectral-function expression (26) does not describe a branch line. Consistently, for finite values of U/t the function $C_{s1, \iota'}(q)$ of Eq. (26) has smaller values than those of the function $C_{s1}(q)$ appearing in expression (22). However, for large values of U/t and bare-momentum values in the vicinity of $\iota' k_F$ such an exponent corresponds to a branch line, as it reaches values smaller than one. We recall that for very small domains around the end points $k = \pm 3k_F$ and $k = \pm 5k_F$ the spectral function is not of the form (26), but instead is of the general form given in Eq. (16).

Equivalent results are obtained for the four $c0, \iota', \iota''$ branch lines, where $\iota', \iota'' = \pm 1$. In this case, the specific form of the general expressions (13) for the points $(k, \omega_{c0, \iota', \iota''}(k))$ belonging to the $c0, \iota', \iota''$ branch lines in the $m \rightarrow 0$ limit, corresponds to $k_0 = \iota' 2k_F - \iota'' k_F$ and $l = c_1 = -c_{c0} = -1$ and reads,

$$q = k + \iota' 2k_F - \iota'' k_F; \quad \omega_{c0, \iota', \iota''}(q) = -\epsilon_{c0}(q). \quad (28)$$

The $c0, +1, +1$ branch line, $c0, -1, -1$ branch line, and $c0, -1, +1$ branch line are labeled c, c' , and c'' in Fig. 1, respectively, where they are represented for $k > 0$ and $\omega \leq 0$. In this case the value of the functional (12) is given by the $m \rightarrow 0$ limit of the following parameter,

$$2\Delta_{\alpha\nu}^{\iota}(q) = \left\{ -\iota \left[\frac{1}{2} - \delta_{\iota, \iota'} \right] \delta_{\alpha\nu, c0} - \iota \frac{\xi_{\alpha\nu s1}^0}{2} - \iota'' \frac{\xi_{\alpha\nu s1}^1}{2} - \Phi_{\alpha\nu, c0}(\iota q_{F\alpha\nu}^0, q) \right\}^2; \quad \alpha\nu = c0, s1. \quad (29)$$

The dependence of this quantity on the momentum k is obtained by combining Eqs. (28) and (29). From use of the general expression (14) in the $m \rightarrow 0$ limit, we find the following expression for the one-electron removal spectral function,

$$B^{-1}(k, \omega) \approx C_{c0, \iota', \iota''}(q) \left(\frac{-[\omega + \omega_{c0, \iota', \iota''}(q)]}{4\pi\sqrt{v_{c0} v_{s1}}} \right)^{\zeta_{c0, \iota', \iota''}(q)}. \quad (30)$$

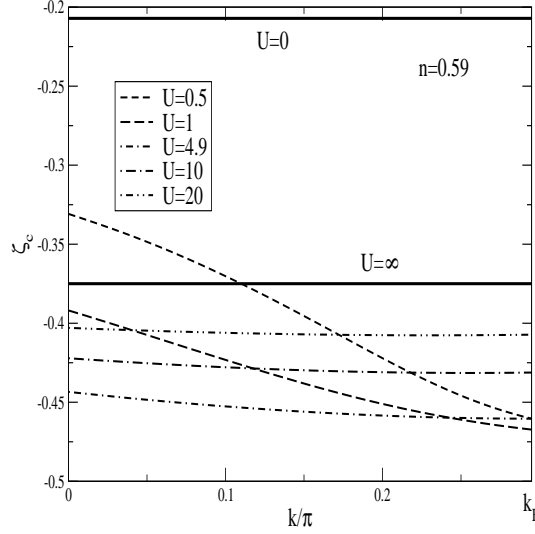


FIG. 3: Momentum dependence of the exponent (31) along the one-electron removal $c \equiv c_0, +1, +1$ branch line of Fig. 1 for $0 < k < k_F$. In the figure that exponent is called ζ_c and is given by $-1/\sqrt{2} + 1/2$ and $-3/8$ for $U/t \rightarrow 0$ and $U/t \rightarrow \infty$, respectively. We note that for a very small momentum domain around $k = k_F$, which corresponds to a branch-line end point, this exponent does not apply, once the spectral function is of the form given in Eq. (16).

This expression corresponds to energy values just below the branch lines. In this expression and in the exponent expressions provided below, the bare-momentum values are in the range $-2k_F < q < 2k_F$. Furthermore, the corresponding momentum values belong to the domains $-3k_F < k < k_F$ and $-k_F < k < 3k_F$ for $\iota' = \iota'' = 1$ and $\iota' = \iota'' = -1$, respectively, and $-5k_F < k < -k_F$ and $k_F < k < 5k_F$ for $\iota' = -\iota'' = 1$ and $\iota' = -\iota'' = -1$, respectively. In the $m \rightarrow 0$ limit, the exponent $\zeta_{c_0, \iota', \iota''}(q)$ of expression (30) reads,

$$\begin{aligned} \zeta_{c_0, \iota', \iota''}(q) &= -1 + \sum_{\alpha\nu=c_0, s_1} \sum_{\iota=\pm 1} \left\{ \left[\frac{1}{2} - \delta_{\iota, \iota'} \right] \delta_{\alpha\nu, c_0} + \frac{\xi_{\alpha\nu s_1}^0}{2} + \iota \iota'' \frac{\xi_{\alpha\nu s_1}^1}{2} + \iota \Phi_{\alpha\nu, c_0}(\iota q_{F\alpha\nu}^0, q) \right\}^2 \\ &= -1 + \sum_{\iota=\pm 1} \left\{ \frac{1}{2} - \delta_{\iota, \iota'} + \iota \iota'' \frac{\xi_0}{4} + \iota \Phi_{c_0, c_0}(\iota 2k_F, q) \right\}^2 \\ &\quad + \sum_{\iota=\pm 1} \left\{ \frac{1}{\sqrt{2}} \left(1 + \frac{\iota \iota''}{2} \right) + \iota \Phi_{s_1, c_0}(\iota k_F, q) \right\}^2. \end{aligned} \quad (31)$$

The exponents $\zeta_{c_0, +1, +1}(q)$ and $\zeta_{c_0, -1, -1}(q)$ of Eq. (31) are negative for all values of momentum and are plotted in Figs. 3 and 4, respectively, as a function of the momentum k for $k > 0$, several values of U/t , and electronic density $n = 0.59$. In these figures these exponents are called ζ_c and $\zeta_{c'}$, respectively. Correspondingly, the weight distribution (30) describes a singular branch line. The exponents $\zeta_{c_0, +1, -1}$ and $\zeta_{c_0, -1, +1}$ of Eq. (31) are positive and smaller than one for all values of momentum and thus in this case the spectral-function expression (30) describes edge branch lines. For finite values of U/t the functions $C_{c_0, \pm 1, \mp 1}(q)$ have in general smaller values than the functions $C_{c_0, \pm 1, \pm 1}(q)$. Moreover, for finite values of U/t $C_{c_0, +1, +1}(q)$ and $C_{c_0, -1, -1}(q)$ are decreasing and increasing functions of k , respectively, whose values are smallest for the domains $-3k_F < k < -2k_F$ and $2k_F < k < 3k_F$, respectively. Again, for very small domains around the end points $k = \pm k_F$, $k = \pm 3k_F$, and $k = \pm 5k_F$ the spectral function is not of the form (30), but instead is of the general form given in Eq. (16).

B. THE ONE-ELECTRON ADDITION LHB BRANCH LINES

For the $n = 1$ half-filling Mott-Hubbard insulator phase there is no LHB. For the $0 < n < 1$ metallic phase, the energy spectrum generated by the LHB one-electron addition excitations is gapless relative to the ground state. The dominant transitions refer to excited energy eigenstates that belong to the subspace whose pseudofermion number deviations are given in Eq. (7). These transitions generate six LHB one-electron addition branch lines whose location in the (k, ω) -plane is shown in the Fig. 1 for $0 < \omega < E_u$. There are two s_1 branch lines which connect the points

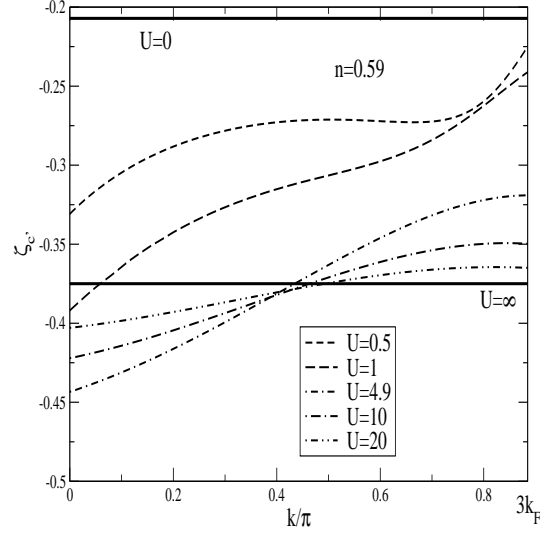


FIG. 4: Momentum dependence of the exponent (31) along the one-electron removal charge $c' \equiv c_0, -1, -1$ branch line of Fig. 1 for $0 < k < 3k_F$. In the figure that exponent is called $\zeta_{c'}$ and is given by $-1/\sqrt{2} + 1/2$ and $-3/8$ for $U/t \rightarrow 0$ and $U/t \rightarrow \infty$, respectively. For a very small momentum domain around $k = 3k_F$, which corresponds to a branch-line end point, this exponent does not apply, since the spectral function is of the form given in Eq. (16).

($k = k_F, \omega = 0$) and ($k = 3k_F, \omega = 0$) and the points ($k = -3k_F, \omega = 0$) and ($k = -k_F, \omega = 0$), respectively. In addition, there are two c_0, ι' branch lines for momentum values $k > 0$ and two for momentum values $k < 0$ such that $k_F < |k| \leq \pi - k_F$ and $3k_F < |k| \leq \pi + k_F$, respectively.

We start by studying the spectral-weight distribution corresponding to the two s_1, ι' branch lines. The specific form of the general expressions (13) for the points ($k, \omega_{s_1, \iota'}(k)$) belonging to such a branch line in the $m \rightarrow 0$ limit, corresponds to $k_0 = \iota' 2k_F$ and $l = -c_1 = c_{s_1} = 1$ and reads,

$$q = \iota' 2k_F - k; \quad \omega_{s_1, \iota'}(q) = -\epsilon_{s_1}(q). \quad (32)$$

The $s_1, +1$ branch line is labeled s in Fig. 1, where it connects the points ($k = k_F, \omega = 0$) and ($k = 3k_F, \omega = 0$) for $\omega \geq 0$. In this case the value of the functional (12) is given by the $m \rightarrow 0$ limit of the following parameter,

$$2\Delta_{\alpha\nu}^{\iota'}(q) = \left\{ \iota \frac{\xi_{\alpha\nu c_0}^0 + \xi_{\alpha\nu s_1}^0}{2} + \iota' \frac{\xi_{\alpha\nu c_0}^1}{2} - \Phi_{\alpha\nu, s_1}(\iota q_{F\alpha\nu}^0, q) \right\}^2; \quad \alpha\nu = c_0, s_1, \quad (33)$$

where as in previous expressions the two-pseudofermion phase shifts are defined in Sec. II and Ref. [17] and the remaining parameters in Eq. (36) of Ref. [19]. Use of the general expression (14) in the $m \rightarrow 0$ limit, leads to the following expression for the LHB one-electron addition spectral function,

$$B^{+1}(k, \omega) \approx C_{s_1, \iota'}^i(q) \left(\frac{\omega - \omega_{s_1, \iota'}(q)}{4\pi \sqrt{v_{c_0} v_{s_1}}} \right)^{\zeta_{s_1, \iota'}^i(q)}, \quad (34)$$

where here and below the index i in the q dependent exponent and multiplicative function whose general expressions are given in Eq. (15), $\zeta_{s_1, \iota'}^i(q)$ and $C_{s_1, \iota'}^i(q)$, respectively, stands for inverse-photoemission and thus indicates that the spectral function corresponds to electron addition, $l = +1$. Moreover, here and in the exponent expressions below, the bare-momentum is in the range $-k_F < q < k_F$ and the corresponding momentum belongs to the domains $k_F < k < 3k_F$ and $-3k_F < k < -k_F$ for $\iota' = 1$ and $\iota' = -1$, respectively. In the $m \rightarrow 0$ limit we find the following exponent,

$$\begin{aligned} \zeta_{s_1, \iota'}^i(q) &= -1 + \sum_{\alpha\nu=c_0, s_1} \sum_{\iota=\pm 1} \left\{ \frac{\xi_{\alpha\nu c_0}^0 + \xi_{\alpha\nu s_1}^0}{2} + \iota \iota' \frac{\xi_{\alpha\nu c_0}^1}{2} - \iota \Phi_{\alpha\nu, s_1}(\iota q_{F\alpha\nu}^0, q) \right\}^2 \\ &= -1 + \sum_{\iota=\pm 1} \left\{ \frac{1}{2\xi_0} + \iota \iota' \frac{\xi_0}{2} - \iota \Phi_{c_0, s_1}(\iota 2k_F, q) \right\}^2 + \sum_{\iota=\pm 1} \left\{ \frac{1}{2\sqrt{2}} - \iota \Phi_{s_1, s_1}(\iota k_F, q) \right\}^2. \end{aligned} \quad (35)$$

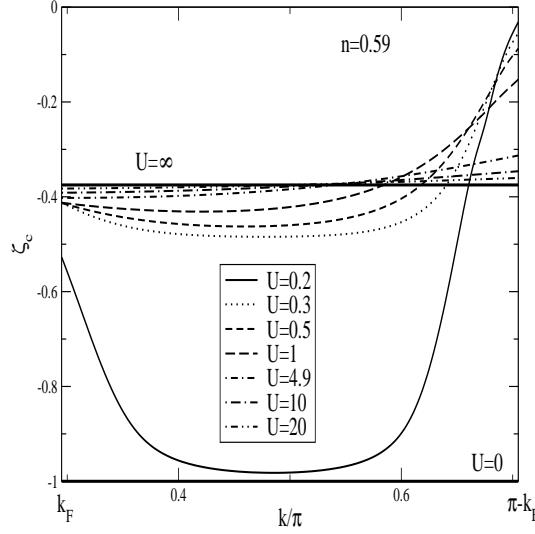


FIG. 5: Momentum dependence of the exponent (39) along the one-electron addition charge $c \equiv c_0, +1$ branch line of Fig. 1 for $k_F < k < \pi - k_F$. In the figure that exponent is called ζ_c and is given by $-3/8$ for $U/t \rightarrow \infty$. For a very small momentum domain around $k = k_F$, which corresponds to a branch-line end point, this exponent does not apply, since the spectral function is of the form given in Eq. (16).

For finite values of U/t , the exponents $\zeta_{s1, \pm 1}^i$ of Eq. (35) are negative for momentum values k such that $|k| \in (k_F, k_*)$ and become positive but smaller than one for $|k| \in (k_*, 3k_F)$. The value of the momentum k_* , changes continuously from $k_* = k_F$ for $U/t \rightarrow 0$ to $k_* = 2k_F$ as $U/t \rightarrow \infty$. It follows that for the $k > 0$ momentum domains $k \in (k_F, k_*)$ and $k \in (k_*, 3k_F)$, the spectral-function expression (34) describes singular and edge branch lines, respectively. The same holds for the corresponding $k < 0$ domains. For finite values of U/t the function $C_{s1, \nu}^i(q)$ is finite for all values of q . The exponent $\zeta_{s1, +1}^i$ is plotted in Fig. 2 as a function of k for $k > 0$, several values of U/t , and electronic density $n = 0.59$. The exponent ζ_s of the figure is the exponent $\zeta_{s1, +1}^i$ of Eq. (35) for momentum values $k_F < k < 3k_F$, whereas for $0 < k < k_F$ ζ_s corresponds to the one-electron removal exponent of Eq. (23).

Similar results are obtained for the c_0, ν'' branch lines. In this case the specific form of the general expressions (13) for the points $(k, \omega_{c0, \nu''}(k))$ belonging to the c_0, ν'' branch lines in the $m \rightarrow 0$ limit, corresponds to $k_0 = -\nu'' k_F$ and $l = c_1 = c_{c0} = 1$ and reads,

$$q = \nu'' k_F + k; \quad \omega_{c0, \nu''} = \epsilon_{c0}(q). \quad (36)$$

The $c_0, +1$ and $c_0, -1$ branch lines are labeled c and c' in Fig. 1, respectively, where they are represented for $k > 0$ momentum values such that $k_F < k \leq \pi - k_F$ and $3k_F < k \leq \pi + k_F$, respectively, for $\omega \geq 0$. In this case the value of the functional (12) is given by the $m \rightarrow 0$ limit of the following parameter,

$$2\Delta_{\alpha\nu}^{\nu}(q) = \left\{ -\nu'' \frac{\xi_{\alpha\nu s1}^1}{2} + \Phi_{\alpha\nu, c0}(\nu q_{F\alpha\nu}^0, q) \right\}^2; \quad \alpha\nu = c0, s1. \quad (37)$$

The k -dependence of this quantity is obtained by combining Eqs. (36) and (37). From use of the general expression (14), in the $m \rightarrow 0$ limit, we find the following expression for the LHB one-electron addition spectral function,

$$\begin{aligned} B^{+1}(k, \omega) &\approx C_{c0, \nu''}^i(q) \left(\frac{\omega - \omega_{c0, \nu''}(q)}{4\pi\sqrt{v_{c0} v_{s1}}} \right)^{\zeta_{c0, \nu''}^i(q)}; \quad \zeta_{c0, \nu''}^i(q) > -1, \\ &= \delta(\omega - \omega_{c0, \nu''}(k)); \quad \zeta_{c0, \nu''}^i(q) = -1. \end{aligned} \quad (38)$$

Here the bare-momentum is in the range $2k_F < |q| \leq \pi$. Moreover, the momentum is such that $k_F < k \leq \pi - k_F$ and $3k_F < k \leq \pi + k_F$ for $k > 0$ and $\nu'' = 1$ and $\nu'' = -1$, respectively. For $k < 0$, it is such that $-\pi + k_F \leq k < -k_F$ and $-\pi - k_F \leq k < -3k_F$ for $\nu'' = -1$ and $\nu'' = 1$, respectively. In the $m \rightarrow 0$ limit, the exponent of expression (38) reads,

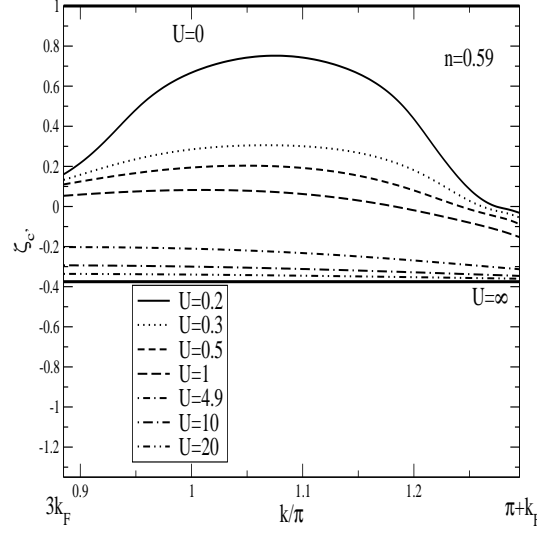


FIG. 6: Momentum dependence of the exponent (39) along the one-electron addition charge $c' \equiv c0, -1$ branch line of Fig. 1 for $3k_F < k < \pi + k_F$. In the figure that exponent is called $\zeta_{c'}$ and is given by $-3/8$ for $U/t \rightarrow \infty$. For a very small momentum domain around $k = 3k_F$, which corresponds to a branch-line end point, this exponent does not apply, since the spectral function is of the form given in Eq. (16).

$$\begin{aligned} \zeta_{c0, \iota''}^i(q) &= -1 + \sum_{\alpha\nu=c0, s1} \sum_{\iota=\pm 1} \left\{ -\iota \iota'' \frac{\xi_{\alpha\nu s1}^1}{2} + \iota \Phi_{\alpha\nu, c0}(\iota q_{F\alpha\nu}^0, q) \right\}^2 \\ &= -1 + \sum_{\iota=\pm 1} \left\{ -\iota \iota'' \frac{\xi_0}{4} + \iota \Phi_{c0, c0}(\iota 2k_F, q) \right\}^2 + \sum_{\iota=\pm 1} \left\{ -\iota \iota'' \frac{1}{2\sqrt{2}} + \iota \Phi_{s1, c0}(\iota k_F, q) \right\}^2. \end{aligned} \quad (39)$$

The exponent $\zeta_{c0, +1}$ of Eq. (39) is negative for all values of momentum and is plotted in Fig. 5 as a function of k for $k > 0$, several values of U/t , and electronic density $n = 0.59$. In that figure the exponent $\zeta_{c0, +1}$ is called ζ_c . So the corresponding spectral-function expression (38) describes a singular branch line. The exponent $\zeta_{c0, -1}$ of Eq. (39) is negative for intermediate and large values of U/t and positive for small values of U/t . It is plotted in Fig. 6 as a function of k for $k > 0$, several values of U/t , and electronic density $n = 0.59$. In this figure the exponent $\zeta_{c0, -1}$ is called $\zeta_{c'}$. Except in the vicinity of the branch-line end point, the function $C_{c0, +1}^i(q)$ is finite for its q domain and larger than the function $C_{c0, -1}^i(q)$.

C. THE ONE-ELECTRON ADDITION UHB BRANCH LINES

The ground-state transitions to the excited energy eigenstates belonging to the subspace whose pseudofermion number deviations are given in Eq. (8), generate several UHB electron addition branch lines whose location in the (k, ω) -plane is shown in the Fig. 1 for $\omega > E_u$. Such transitions have a minimum energy given by the finite energy correlation parameter $E_u = 2\mu$ defined in Ref. [19], whose limiting values are provided in Eq. (6). At half-filling the energy E_u equals the Mott-Hubbard gap E_{MH} and the suitable pseudofermion and $-1/2$ Yang holon number deviations associated with the electron-addition UHB are those given in Eq. (9). The spectral weight generated by transitions to the subspace with number deviations given in that equation vanishes for finite values of the doping concentration $\delta = [1 - n]$, as mentioned above and confirmed in Ref. [25]. On the other hand, for small finite values of $(N_a - N^0)$ there is a competition between the two types of excited energy eigenstates associated with the number deviations of Eqs. (8) and (9), respectively. (Here N^0 denotes the initial-ground-state electron number.) For half-filling, where $N_a = N^0$, the transitions to the excited states whose pseudofermion number deviations are given in Eqs. (8) are not allowed. Moreover, at half-filling there is no LHB, as mentioned above.

For the metallic phase, the UHB one-electron addition spectral function has three $s1$ pseudofermion branch lines, four $c0$ pseudofermion branch lines, and four $c1$ pseudofermion branch lines, whose location in the (k, ω) -plane is shown in Fig. 1. The half-filling UHB one-electron addition spectral function has no $c1$ pseudofermion branch lines. The shape of the UHB one-electron addition $s1$ and $c0$ pseudofermion branch lines is obtained from the one-electron

removal $s1$ and $c0$ pseudofermion branch lines, respectively, by the transformation $k \rightarrow \pi - k$ and $\omega \rightarrow E_u - \omega$ for $\omega \leq 0$.

For the UHB one-electron addition spectral function, it is convenient to use a momentum representation centered at momentum π instead of zero momentum. The shape of the $c0$ and $s1$ branch lines is obtained from the corresponding one-electron removal branch lines by use of the above procedure. There is a $s1_u$ branch line, two $s1_u, l'$ branch lines, and four $c0_u, l', l''$ branch lines. These correspond to the one-electron removal $s1$ branch line, two $s1, l'$ branch lines, and four $c0, l', l''$ branch lines, respectively, studied above. Some of these UHB lines are labeled by s_u, c_u, c'_u , and c''_u in Fig. 1. We find below that the exponents that control the spectral-weight distribution in the vicinity of these lines are the same as the corresponding one-electron removal exponents. In addition, we study the four $c1, l', l''$ branch lines. All these lines are labeled by $c1$ in Fig. 1. The $c1, +1, -1$ (and $c1, -1, +1$) branch line connects the points $(k = -\pi + k_F, \omega = E_u)$ and $(k = \pi - 3k_F, \omega = E_u)$ (and the points $(k = -\pi + 3k_F, \omega = E_u)$ and $(k = \pi - k_F, \omega = E_u)$), and the $c1, +1, +1$ (and $c1, -1, -1$) branch line connects the points $(k = -\pi - k_F, \omega = E_u)$ and $(k = \pi - 5k_F, \omega = E_u)$ (and the points $(k = -\pi + 5k_F, \omega = E_u)$ and $(k = \pi + k_F, \omega = E_u)$).

At half-filling the UHB one-electron addition spectrum is fully generated from the corresponding one-electron removal spectrum by the transformation $k \rightarrow \pi - k$ and $\omega \rightarrow E_{MH} - \omega$ for $\omega \leq 0$. Thus, for the Mott-Hubbard insulator phase, the symmetry $B^{-1}(k, \omega) = B^{+1}(\pi - k, E_u - \omega) = B^{+1}(\pi - k, E_{MH} - \omega)$ is valid for all values of momentum k and energy $\omega \leq 0$. Here, we defined the zero-energy level at the lower limit of the Mott-Hubbard gap. At half-filling, one usually defines such an energy level at the middle of the Mott-Hubbard gap. For such a case the symmetry becomes $B^{-1}(k, \omega) = B^{+1}(\pi - k, -\omega)$ for $\omega \leq 0$. However, for finite values of the doping concentration, there is a small decrease in the amount of one-electron spectral weight relative to that located on the $c0$ and $s1$ pseudofermion branch lines of the one-electron removal spectrum. For the UHB one-electron addition spectrum the small weight fraction corresponding to such a decrease appears transferred over to the $c1$ pseudofermion edge branch lines and other weaker spectral-weight structures generated by the $c1$ pseudofermion creation. Nevertheless, there remains some relation between the one-electron removal spectrum and the UHB one-electron addition spectrum under the transformation $k \rightarrow \pi - k$ and $\omega \rightarrow E_u - \omega$ for $\omega \leq 0$. For instance and as mentioned above, that transformation fully defines the shape of the UHB $s1_u$ branch line, two $s1_u, l'$ branch lines, and four $c0_u, l', l''$ branch lines, whose intensity for the metallic phase is slightly smaller for the UHB relative to the corresponding removal branch lines. Moreover, below we confirm that the exponents associated with such UHB branch lines are precisely the same as for the corresponding one-electron removal branch lines. The value of the momentum dependent function $C_{\alpha\nu}(q)$ of Eq. (15), which appears in the power-law spectral-function expression of Eq. (14), is in general smaller for the UHB one-electron addition branch lines.

We start by the evaluation of the spectral-weight distribution corresponding to the $s1_u$ branch line. The specific form of the general expressions (13) for the points $(k, \omega_{s1_u}(k))$ belonging to such a branch line in the $m \rightarrow 0$ limit, corresponds to $k_0 = \pi$ and $l = -c_1 = c_s = 1$ and reads,

$$q = \pi - k; \quad \omega_{s1_u} = E_u - \epsilon_{s1}(q). \quad (40)$$

In figure 1 the $s1_u$ branch line is labeled by s_u , where it connects the points $(k = \pi - k_F, \omega = E_u)$ and $(k = \pi + k_F, \omega = E_u)$ for $\omega \geq E_u$. The value of the functional (12) is a function of q which has precisely the same form as Eq. (21). The only difference is that in the present case the bare-momentum q obeys Eq. (40), which is different from the corresponding Eq. (20). Direct use of the general expression (14) in the $m \rightarrow 0$ limit, leads to the following expression for the UHB one-electron addition spectral function,

$$\begin{aligned} B^{+1}(k, \omega) &\approx C_{s1_u}^i(q) \left(\frac{\omega - \omega_{s1_u}(q)}{4\pi\sqrt{v_{c0}v_{s1}}} \right)^{\zeta_{s1_u}^i(q)}; \quad \zeta_{s1_u}^i(q) > -1 \\ &= \delta(\omega - \omega_{s1_u}(k)); \quad \zeta_{s1_u}^i(q) = -1. \end{aligned} \quad (41)$$

This expression corresponds to $-k_F < q < k_F$ and $\pi - k_F < k < \pi + k_F$. In the limit $m \rightarrow 0$, we find that $\zeta_{s1_u}^i(q) = \zeta_{s1}(q)$, where the exponent $\zeta_{s1}(q)$ is given in Eq. (23) and is plotted as a function of the momentum in Fig. 2 for $0 < k < k_F$. This confirms that the UHB one-electron addition exponent $\zeta_{s1_u}^i(q)$ equals the corresponding one-electron removal exponent (23). However, based on the general $C_{\alpha\nu}(q)$ expression given in Eq. (15) we find that for finite values of the doping concentration the momentum-dependent function $C_{s1_u}^i(q)$ is slightly smaller than the corresponding function $C_{s1}(q)$ on the right-hand side of Eq. (22).

In the $m \rightarrow 0$ limit, the energy pseudogap,

$$\Delta_{UHB-LHB} = [E_u - \epsilon_{c0}(\pi)], \quad (42)$$

plays an important role. On the right-hand side of Eq. (42) $\epsilon_{c0}(\pi)$ is the $c1$ pseudofermion energy band given in Eq. (C.15) of Ref. [15] for $q = \pi$ and E_u is the correlation energy $E_u = 2\mu$ defined in Ref. [19], whose limiting values are provided in Eq. (6). This energy pseudogap corresponds in the metallic phase, to the minimum value of the energy that at fixed momentum k separates in the (k, ω) -plane the UHB one-electron addition $s1_u$ branch line from the LHB one-electron addition $c0, \iota'$ branch line such that $\text{sgn}(k) \iota' = 1$. The energy pseudogap (42) is always finite for $U/t > 0$, but vanishes for all electronic densities as $U/t \rightarrow 0$. It corresponds to the momentum values $k = \pm[\pi - k_F]$ (see Fig. 1). At half-filling this energy equals the Mott-Hubbard and corresponds to the momentum values $k = \pm k_F = \pm\pi/2$.

Next, we consider the weight distribution corresponding to the $s1_u, \iota'$ branch lines. The specific form of the general expressions (13), for the points $(k, \omega_{s1_u, \iota'}(k))$ belonging to such branch lines, in the $m \rightarrow 0$ limit, corresponds to $k_0 = \pi + \iota' 4k_F$ and $l = -c_1 = c_{s1} = 1$ and reads,

$$q = \pi + \iota' 4k_F - k; \quad \omega_{s1_u, \iota'}(k) = E_u - \epsilon_{s1}(q). \quad (43)$$

A small portion of the $s1_u, +1$ branch line appears in Fig. 1 for momentum values k such that $\pi + 3k_F < k < 3\pi - 3k_F$ and $\omega \geq E_u$. In this case the value of the functional (12) is a function of q , which has precisely the same form as that of Eq. (33). The only difference is that here the bare-momentum q obeys Eq. (43), which is different from the corresponding Eq. (24). Direct use of the general expression (14) in the $m \rightarrow 0$ limit, leads to the following expression for UHB one-electron addition spectral function,

$$B^{+1}(k, \omega) \approx C_{s1_u, \iota'}^i(q) \left(\frac{\omega - \omega_{s1_u, \iota'}(q)}{4\pi \sqrt{v_{c0} v_{s1}}} \right)^{\zeta_{s1_u, \iota'}^i(q)}, \quad (44)$$

which corresponds to $-k_F < q < k_F$ and $\pi + 3k_F < k < \pi + 5k_F$ and $\pi - 5k_F < k < \pi - 3k_F$ for $\iota' = 1$ and $\iota' = -1$, respectively. In the limit $m \rightarrow 0$, we find that $\zeta_{s1_u, \iota'}^i(q) = \zeta_{s, \iota'}(q)$, where the exponent $\zeta_{s, \iota'}(q)$ is given in Eq. (27) and the function $C_{s1_u, \iota'}^i(q)$ is slightly smaller than that corresponding to that exponent.

Equivalent results are obtained for the $c0_u, \iota', \iota''$ branch lines. In this case the specific form of the general expressions (13) for the points $(k, \omega_{c0_u, \iota', \iota''}(k))$ belonging to the $c0_u, \iota', \iota''$ branch lines in the $m \rightarrow 0$ limit, corresponds to $k_0 = \pi + \iota' 2k_F - \iota'' k_F$ and $l = -c_1 = c_{c0} = 1$ and is given by,

$$q = \pi + \iota' 2k_F - \iota'' k_F - k; \quad \omega_{c0_u, \iota', \iota''}(k) = E_u - \epsilon_{c0}(q). \quad (45)$$

Some of these branch lines are labeled c_u, c'_u , and c''_u in Fig. 1. In this case the value of the functional (12) is a function of the bare-momentum q which equals the function given in Eq. (29). From use of the general expression (14), in the $m \rightarrow 0$ limit, we find the following expression for the UHB one-electron addition spectral function,

$$B^{+1}(k, \omega) \approx C_{c0_u, \iota', \iota''}^i(q) \left(\frac{\omega - \omega_{c0_u, \iota', \iota''}(q)}{4\pi \sqrt{v_{c0} v_{s1}}} \right)^{\zeta_{c0_u, \iota', \iota''}^i(q)}. \quad (46)$$

This expression corresponds to $-2k_F < q < 2k_F$. The momentum values are in the ranges $\pi - k_F < k < \pi + 3k_F$ and $\pi - 3k_F < k < \pi + k_F$ for $\iota' = \iota'' = 1$ and $\iota' = \iota'' = -1$, respectively. For $\iota' = -\iota'' = 1$ and $\iota' = -\iota'' = -1$ the momentum values are such that $\pi + k_F < k < \pi + 5k_F$ and $\pi - 5k_F < k < \pi - k_F$, respectively. In expression (46), the exponent reads $\zeta_{c0_u, \iota', \iota''}^i(q) = \zeta_{c0, \iota', \iota''}(q)$, where the exponent $\zeta_{c0, \iota', \iota''}(q)$ is given in Eq. (31). (The exponents $\zeta_{c0, +1, +1}$ and $\zeta_{c0, -1, -1}$ are plotted in Figs. 3 and 4, respectively, as a function of k for $k > 0$.) This relation is consistent with the UHB one-electron addition exponent $\zeta_{c0_u, \iota', \iota''}^i(q)$ equaling the corresponding one-electron removal exponent (31). However, for finite values of the doping concentration, the momentum-dependent constant $C_{c0_u, \iota', \iota''}^i(q)$ is slightly smaller than the corresponding constant $C_{c0, \iota', \iota''}(q)$ on the right-hand side of Eq. (30).

We thus conclude that the $s1_u$ branch line, $s1_u, \iota'$ branch lines, and $c0_u, \iota', \iota''$ branch lines of the UHB, one-electron removal spectral function are controlled by the same exponents as the $s1$ branch line, $s1, \iota'$ branch lines, and $c0, \iota', \iota''$ branch lines, respectively, of the one-electron removal spectral function. However, except at half-filling the spectral weight associated with these UHB branch lines for finite values of U/t is in general smaller than the weight associated with the corresponding lines of the one-electron removal spectral function. This is because away from half-filling the UHB spectral weight also spreads around $c1$ pseudofermion edge branch lines, which do not exist for the one-electron removal spectral function.

Finally, let us study the UHB weight distribution corresponding to the $c1, \iota', \iota''$ edge branch lines. (These lines do not occur for $n = 1$.) The specific form of the general expression (13) for the points $(k, \omega_{c1, \iota', \iota''}(k))$ belonging to the

$c1, \iota', \iota''$ branch lines, in the $m \rightarrow 0$ limit, corresponds to $k_0 = -\text{sgn}(q)\pi - \iota' 2k_F - \iota'' k_F$ and $l = c_1 = -c_{c1} = 1$ and is given by,

$$q = (1 + \iota')\pi - \iota' 2k_F - \iota'' k_F - k; \quad \omega_{c1, \iota', \iota''} = E_u + \epsilon_{c1}(q). \quad (47)$$

These branch lines are labeled $c1$ in Fig. 1. In this case the value of the functional (12) is given by the $m \rightarrow 0$ limit of the following parameter,

$$2\Delta_{\alpha\nu}^{\iota}(q) = \left\{ -\iota \frac{\xi_{\alpha\nu c0}^0 + \xi_{\alpha\nu s1}^0}{2} - \frac{\iota' \xi_{\alpha\nu c0}^1 + \iota'' \xi_{\alpha\nu s1}^1}{2} + \Phi_{\alpha\nu, c1}(\iota q_{F\alpha\nu}^0, q) \right\}^2; \quad \alpha\nu = c0, s1, \quad (48)$$

where the bare-momentum values are such that $0 \leq |q| < [\pi - 2k_F]$. Use of the general expression (14) in the $m \rightarrow 0$ limit, leads to the following expression for the UHB one-electron addition spectral function,

$$B^{+1}(k, \omega) \approx C_{c1, \iota', \iota''}^i(q) \left(\frac{\omega - \omega_{c1, \iota', \iota''}(q)}{4\pi\sqrt{v_{c0} v_{s1}}} \right)^{\zeta_{c1, \iota', \iota''}^i(q)}. \quad (49)$$

This expression corresponds to bare-momentum values such that $-2k_F < q < 2k_F$. Moreover, the momentum k belongs to the domains $-\pi + 3k_F < k < \pi - k_F$ and $\pi + k_F < k < 3\pi - 3k_F$ for $\iota' = -\iota'' = -1$ and $\iota' = -\iota'' = +1$, respectively, and $-\pi + 5k_F < k < \pi + k_F$ and $\pi - k_F < k < 3\pi - 5k_F$ for $\iota' = \iota'' = -1$ and $\iota' = \iota'' = 1$, respectively. For finite values of U/t , finite values of doping concentration, and in the $m \rightarrow 0$ limit, the exponent reads,

$$\begin{aligned} \zeta_{c1, \iota', \iota''}^i(q) &= -1 + \sum_{\alpha\nu=c0, s1} \sum_{\iota=\pm 1} \left\{ \frac{\xi_{\alpha\nu c0}^0 + \xi_{\alpha\nu s1}^0}{2} + \iota \left(\frac{\iota' \xi_{\alpha\nu c0}^1 + \iota'' \xi_{\alpha\nu s1}^1}{2} \right) - \iota \Phi_{\alpha\nu, c1}(\iota q_{F\alpha\nu}^0, q) \right\}^2 \\ &= -1 + \sum_{\iota=\pm 1} \left\{ \frac{1}{2\xi_0} + \iota(2\iota' + \iota'') \frac{\xi_0}{4} - \iota \Phi_{c0, c1}(\iota 2k_F, q) \right\}^2 \\ &+ \sum_{\iota=\pm 1} \left\{ \frac{1}{2\sqrt{2}}(1 + \iota\iota'') - \iota \Phi_{s1, c1}(\iota k_F, q) \right\}^2. \end{aligned} \quad (50)$$

These exponents are always positive and do not correspond to singular branch lines. For some values of bare-momentum q , these exponents are larger than one and thus the corresponding spectral-function expression (49) does not describe a branch line. Furthermore, the function $C_{c1, \iota', \iota''}^i(q)$ has in general smaller values than the corresponding multiplicative functions of the above UHB $c0$ and $s1$ branch lines.

IV. THE PHASE SHIFTS AND BRANCH-LINE EXPONENTS FOR $U/t \rightarrow 0$ AND $U/t \gg 1$

In order to confirm that the spectral-function expressions obtained in Sec. III in the limits $U/t \rightarrow 0$ and $U/t \rightarrow \infty$ recover the correct behaviors, we start by deriving expressions for the corresponding elementary two-pseudofermion phase shifts for $U/t \rightarrow 0$ and $U/t \gg 1$.

A. THE ELEMENTARY TWO-PSEUDO-FERMION PHASE SHIFTS FOR $U/t \rightarrow 0$ AND $U/t \gg 1$

The evaluation of $m \rightarrow 0$ closed-form expressions for the elementary two-pseudofermion phase shifts $\Phi_{c0, c0}(q, q')$, $\Phi_{c0, s1}(q, q')$, $\Phi_{s1, c0}(q, q')$, $\Phi_{s1, s1}(q, q')$, $\Phi_{c0, c1}(q, q')$, and $\Phi_{s1, c1}(q, q')$ in units of π for the limits of $U/t \rightarrow 0$ and $U/t \gg 1$ involves the use of the ground-state rapidity function expressions given in Ref. [19] and two-pseudofermion phase-shift expressions provided in Eqs. (15) and (A1)-(A13) of Ref. [17]. First, we use the ground-state rapidity function expressions to derive the following closed-form expressions for the ground-state functions $k^0(q)$, $\Lambda_{c0}^0(q)$, $\Lambda_{c\nu}^0(q)$, and $\Lambda_{s1}^0(q)$, valid for zero spin density $m \rightarrow 0$, values of the electronic density $0 \leq n \leq 1$, and limiting on-site repulsion values $U/t \rightarrow 0$ and $U/t \gg 1$,

$$\begin{aligned}
k^0(q) &= \frac{q}{2}; \quad |q| \leq 2k_F, \quad U/t \rightarrow 0; \\
&= \text{sgn}(q) [|q| - k_F]; \quad 2k_F \leq |q| < \pi/a, \quad U/t \rightarrow 0; \\
&= \text{sgn}(q) \pi; \quad |q| = \pi, \quad U/t \rightarrow 0; \\
&= q - \frac{4tn}{U} \ln(2) \sin(q); \quad |q| \leq \pi, \quad U/t \gg 1,
\end{aligned} \tag{51}$$

$$\begin{aligned}
\Lambda_{c0}^0(q) &= \sin\left(\frac{q}{2}\right); \quad |q| \leq 2k_F, \quad U/t \rightarrow 0; \\
&= \text{sgn}(q) \sin(|q| - k_F); \quad 2k_F \leq |q| < \pi, \quad U/t \rightarrow 0; \\
&= 0; \quad |q| = \pi, \quad U/t \rightarrow 0; \\
&= \sin(q) - \frac{2tn}{U} \ln(2) \sin(2q); \quad |q| \leq \pi, \quad U/t \gg 1,
\end{aligned} \tag{52}$$

$$\begin{aligned}
\Lambda_{c\nu}^0(q) &= \text{sgn}(q) \sin\left(\frac{(|q| + \pi n)}{2}\right); \quad 0 < |q| < (\pi - 2k_F), \quad U/t \rightarrow 0 \\
&= 0; \quad q = 0, \quad U/t \rightarrow 0 \\
&= \pm\infty; \quad q = \pm(\pi - 2k_F), \quad U/t \rightarrow 0 \\
&= \frac{\nu U}{4t} \tan\left(\frac{q}{2\delta}\right); \quad 0 \leq |q| \leq (\pi - 2k_F), \quad U/t \gg 1,
\end{aligned} \tag{53}$$

for $\nu > 0$, and

$$\begin{aligned}
\Lambda_{s1}^0(q) &= \sin(q); \quad |q| < k_F, \quad U/t \rightarrow 0 \\
&= \pm\infty; \quad q = \pm k_F, \quad U/t \rightarrow 0 \\
&= \frac{U}{2\pi t} \text{arcsinh}\left(\tan\left(\frac{q}{n}\right)\right); \quad |q| \leq k_F, \quad U/t \gg 1,
\end{aligned} \tag{54}$$

respectively. Second, we use Eqs. (51)-(54) in Eq. (15) of Ref. [17]. By manipulation of the integral equations (A1)-(A13) of the same reference for the limits of zero spin density $m \rightarrow 0$ and $U/t \rightarrow 0$ we find the following expressions for the above bare-momentum two-pseudofermion phase shifts in units of π ,

$$\Phi_{c0, c0}(q, q') = -\frac{\text{sgn}\left(\sin k_{c0}^0(q) - \sin k_{c0}^0(q')\right)}{C_c(q)} + \delta_{|q|, 2k_F} \delta_{q, q'} [\text{sgn}(q)] \left(\frac{3}{2\sqrt{2}} - 1\right), \tag{55}$$

$$\Phi_{c0, s1}(q, q') = -\frac{\text{sgn}\left(\sin k_{c0}^0(q) - c_{s1}(q') \sin(q')\right)}{C_c(q)} + \delta_{|q|, 2k_F} \delta_{q, 2q'} \frac{\text{sgn}(q')}{2\sqrt{2}}, \tag{56}$$

$$\Phi_{s1, c0}(q, q') = -\frac{\text{sgn}\left(c_{s1}(q) \sin(q) - \sin k_{c0}^0(q')\right)}{C_s(q)} - \delta_{|q|, k_F} \delta_{q, q'/2} \frac{\text{sgn}(q)}{2\sqrt{2}}, \tag{57}$$

$$\Phi_{s1, s1}(q, q') = \delta_{|q|, k_F} \frac{\text{sgn}(q)}{2\sqrt{2}} \left[1 + \delta_{q, q'} 2(1 - \sqrt{2})\right], \tag{58}$$

$$\Phi_{c0, c1}(q, q') = -2 \frac{\text{sgn}\left(\sin k_{c0}^0(q) - c_{c1}(q') \sin k_{c1}^0(q')\right)}{C_c(q)}, \tag{59}$$

and

$$\Phi_{s1,c1}(q, q') = -\frac{\Theta(k_F - |q|)}{2} \operatorname{sgn}(\sin q - \sin k_{c1}^0(q')), \quad (60)$$

respectively. Here the sign function is such that $\operatorname{sgn}(0) = 0$ and $\Theta(x) = 1$ for $x > 0$ and $\Theta(x) = 0$ for $x \leq 0$ and thus $\Phi_{s1,c1}(\pm k_F, q') = 0$. In the above equations, $k_{c0}^0(q) = \lim_{U/t \rightarrow 0} k^0(q)$ where the $U/t \rightarrow 0$ value of $k^0(q)$ is given in Eq. (51),

$$\begin{aligned} k_{c1}^0(q) &= \frac{q}{2} + \operatorname{sgn}(q) k_F; \quad 0 < |q| \leq [\pi - 2k_F] \\ &= 0; \quad q = 0, \end{aligned} \quad (61)$$

$$\begin{aligned} C_c(q) &= 2 \left[\Theta(2k_F - |q|) + \sqrt{2} \delta_{|q|, 2k_F} + 2 \Theta(\pi - |q|) \Theta(|q| - 2k_F) + \delta_{|q|, \pi} \right] \\ C_s(q) &= 2 \left[\Theta(k_F - |q|) + \sqrt{2} \delta_{|q|, k_F} \right], \end{aligned} \quad (62)$$

and

$$\begin{aligned} c_{s1}(q) &= 1, \quad |q| < k_F; \quad c_{s1}(q) = \infty, \quad q = \pm k_F \\ c_{c1}(q) &= 1, \quad |q| < [\pi - 2k_F]; \quad c_{c1}(q) = \infty, \quad q = \pm[\pi - 2k_F]. \end{aligned} \quad (63)$$

The $U/t \rightarrow 0$ elementary two-pseudofermion phase shifts defined by Eqs. (55)-(63) are plotted in Ref. [21] as a function of the bare momentum for $n = 0.59$.

By use of similar manipulations we find that for $m \rightarrow 0$ and $U/t \gg 1$ the above elementary two-pseudofermion phase shifts in units of π can be written as,

$$\Phi_{c0,c0}(q, q') = -\frac{(\xi_0 - 1/\xi_0)}{2} \left(\frac{\sin(q) - \sin(q')}{2 \sin(\pi n)} \right) + \left[\frac{(\xi_0 + 1/\xi_0)}{2} - 1 \right] \frac{\sin(q')}{\sin(\pi n)}. \quad (64)$$

$$\Phi_{c0,s1}(q, q') = \frac{1}{2\pi} \arctan \left(\sinh \left(-\frac{2\pi t}{U} \sin(q) + \operatorname{arcsinh} \left(\tan \left(\frac{q'}{n} \right) \right) \right) \right) + \frac{(\xi_0 - 1)}{4} \frac{2q'}{\pi n}, \quad (65)$$

$$\begin{aligned} \Phi_{s1,c0}(q, q') &= -\frac{1}{2\pi} \arctan \left(\sinh \left(\operatorname{arcsinh} \left(\tan \left(\frac{q}{n} \right) \right) - \frac{2\pi t}{U} \sin(q') \right) \right); \quad q \neq \pm k_F \\ &= -\frac{\operatorname{sgn}(q)}{2\sqrt{2}}; \quad q = \pm k_F, \end{aligned} \quad (66)$$

$$\begin{aligned} \Phi_{s1,s1}(q, q') &= \frac{1}{\pi} \int_0^\infty d\omega \frac{\sin \left(\omega \frac{2}{\pi} [\operatorname{arcsinh} \left(\tan \left(\frac{q}{n} \right) \right) - \operatorname{arcsinh} \left(\tan \left(\frac{q'}{n} \right) \right)] \right)}{\omega (1 + e^{2\omega})} \\ &+ \frac{t}{U} \frac{\sin(\pi n)}{2} \frac{2q'}{\pi n} \cos \left(\frac{q}{n} \right); \quad q \neq \pm k_F \\ &= \frac{\operatorname{sgn}(q)}{2\sqrt{2}}; \quad q = \pm k_F, \quad q' \neq \pm k_F \\ &= [\operatorname{sgn}(q)] \left(\frac{3}{2\sqrt{2}} - 1 \right); \quad q = q' = \pm k_F, \end{aligned} \quad (67)$$

$$\Phi_{c0,c1}(q, q') = \frac{1}{\pi} \arctan \left(-\frac{4t}{U} \sin(q) + \tan \left(\frac{q'}{2\delta} \right) \right) + \frac{(\xi_0 - 1)}{2} \frac{q'}{\pi \delta}, \quad (68)$$

and

$$\Phi_{s1, c1}(q, q') = \frac{t}{U} \sin(\pi\delta) \frac{2q'}{\pi\delta} \cos\left(\frac{q}{n}\right), \quad (69)$$

respectively. In equations (64), (65), and (68) the parameter ξ_0 should be replaced by its $U/t \gg 1$ expression provided in Eq. (19). Note that the t/U leading-order term of the quantity $(\xi_0 + 1/\xi_0)$ appearing in Eq. (64) is of second order. However, since the t/U second order term of the parameter ξ_0 , which is not given in Eq. (19), does not contribute to $(\xi_0 + 1/\xi_0)$, that leading-order term should be considered.

For $U/t = 100$ and $n = 0.59$ the bare-momentum dependence of the elementary two-pseudofermion phase-shift expansions (64)-(69) is similar to the exact dependence plotted in the corresponding figures of Ref. [21]. Interestingly, for $U > 4t$ these phase-shift expansions are a reasonably good approximation for the exact phase-shift expressions. For instance, the bare-momentum dependence of the phase-shift expansions (64)-(69) is plotted in Fig. 7 for $n = 0.59$ and $U/t = 4.9$. Comparison with the exact bare-momentum dependence of the corresponding figures of Ref. [21] for $U/t = 4.9$ confirms a remarkable agreement.

B. THE ONE-ELECTRON BRANCH LINES AS $U/t \rightarrow 0$ AND $U/t \rightarrow \infty$

Let us use the above elementary two-pseudofermion phase-shift limiting values given in Eqs. (55)-(69) and the exponent expressions derived in Sec. III to confirm that the momentum and energy dependence of the spectral-weight distribution in the vicinity of the corresponding branch lines in the limits $U/t \rightarrow 0$ and $U/t \rightarrow \infty$, recovers the correct behaviors. All expressions provided below are valid for electronic densities n such that $0 < n < 1$. Although in this paper we use an extended momentum scheme such that $-\infty < k < \infty$, we find below that for $U/t \rightarrow 0$ the correct electronic spectrum has contributions for $-\pi < k < \pi$ from a momentum domain such that $|k| < \pi$.

Independently of the general exponent expressions derived by the PDT of Refs. [18, 19], we also used here the method of Refs. [10, 11, 12] to derive the exponents associated with the one-electron spectral function expressions obtained in these references for $U/t \rightarrow \infty$. The limiting values of the general exponents given in Sec. III fully agree with those obtained for $U/t \rightarrow \infty$ by use of the method of Refs. [10, 11, 12]. Thus, our general U/t expressions are fully consistent with the spectral function expressions obtained in Refs. [10, 11, 12] for $U/t \rightarrow \infty$.

Interestingly, for $U/t \rightarrow 0$ the electronic spectrum is fully obtained from some of the branch lines of general form (14), which lead to δ -function weight distributions. In contrast, the very small (k, ω) -plane regions where the end-point behaviors given in Eqs. (16) and (17) are valid disappear as $U/t \rightarrow 0$.

For the one-electron removal $s1$ branch line expression (22), the function $C_{s1}(q)$ gives rise to the weight constant of the δ -peak spectral function of the second expression of Eq. (14). That weight constant arises as $U/t \rightarrow 0$ and is given by $(1/N_a)^{\zeta_0(q)} \rightarrow 1$ [19]. Its independence on the value of the bare momentum q results from the behavior of the functional $\zeta_0(q)$ such that $\zeta_0(q) \rightarrow 0$ as $U/t \rightarrow 0$. We find that in the limits $U/t \rightarrow 0$ and $U/t \rightarrow \infty$, the corresponding exponent (23) reads,

$$\zeta_{s1}(q) = -1, \quad U/t \rightarrow 0; \quad \zeta_{s1}(q) = -\frac{1}{2} + 2\left(\frac{q}{4k_F}\right)^2, \quad U/t \rightarrow \infty, \quad (70)$$

for the q and k values of the spectral-function expression (22). Moreover, according to Eq. (A2) of Ref. [16], in the limit $U/t \rightarrow 0$ the dispersion $\epsilon_{s1}(q)$ becomes the electronic spectrum $\epsilon_{s1}(q) = -2t[\cos(q) - \cos(k_F)]$. Consistently, according to Eq. (70), the exponent (23) is such that $\zeta_{s1}(q) \rightarrow -1$ as $U/t \rightarrow 0$ for all values of q in the range $0 < |q| < k_F$ and thus of the momentum k in the domain $0 < |k| < k_F$. Then, following the second expression of Eq. (22), the correct non-interacting one-electron removal spectral function is reached in this limit.

For the one-electron removal $s1, \iota'$ branch line expression (26), the multiplicative function is such that $C_{s1, \iota'}(q) \rightarrow 0$ as $U/t \rightarrow 0$. Thus, such a branch line does not exist for $U/t \rightarrow 0$, which is the correct result. For $m \rightarrow 0$ and in the limits $U/t \rightarrow 0$ and $U/t \rightarrow \infty$ the corresponding exponent (27) reads,

$$\zeta_{s1, \iota'}(q) = 3, \quad U/t \rightarrow 0; \quad \zeta_{s1, \iota'}(q) = \frac{3}{2} - \iota' \frac{q}{k_F} + 2\left(\frac{q}{4k_F}\right)^2, \quad U/t \rightarrow \infty, \quad (71)$$

for the q and k values of the spectral-function expression (26). In the limit $U/t \rightarrow \infty$, this exponent is such that $\zeta_{s1, \iota'}(q) = 5/8$ for $q \rightarrow \iota' k_F$, $\zeta_{s1, \iota'}(q) = 3/2$ for $q = 0$, and $\zeta_{s1, \iota'}(q) = 21/8$ for $q \rightarrow -\iota' k_F$. For the one-electron removal $c0, \iota', \iota''$ branch line expression (30), the multiplicative function is such that $C_{c0, \iota', \iota''}(q) \rightarrow 0$ as $U/t \rightarrow 0$,

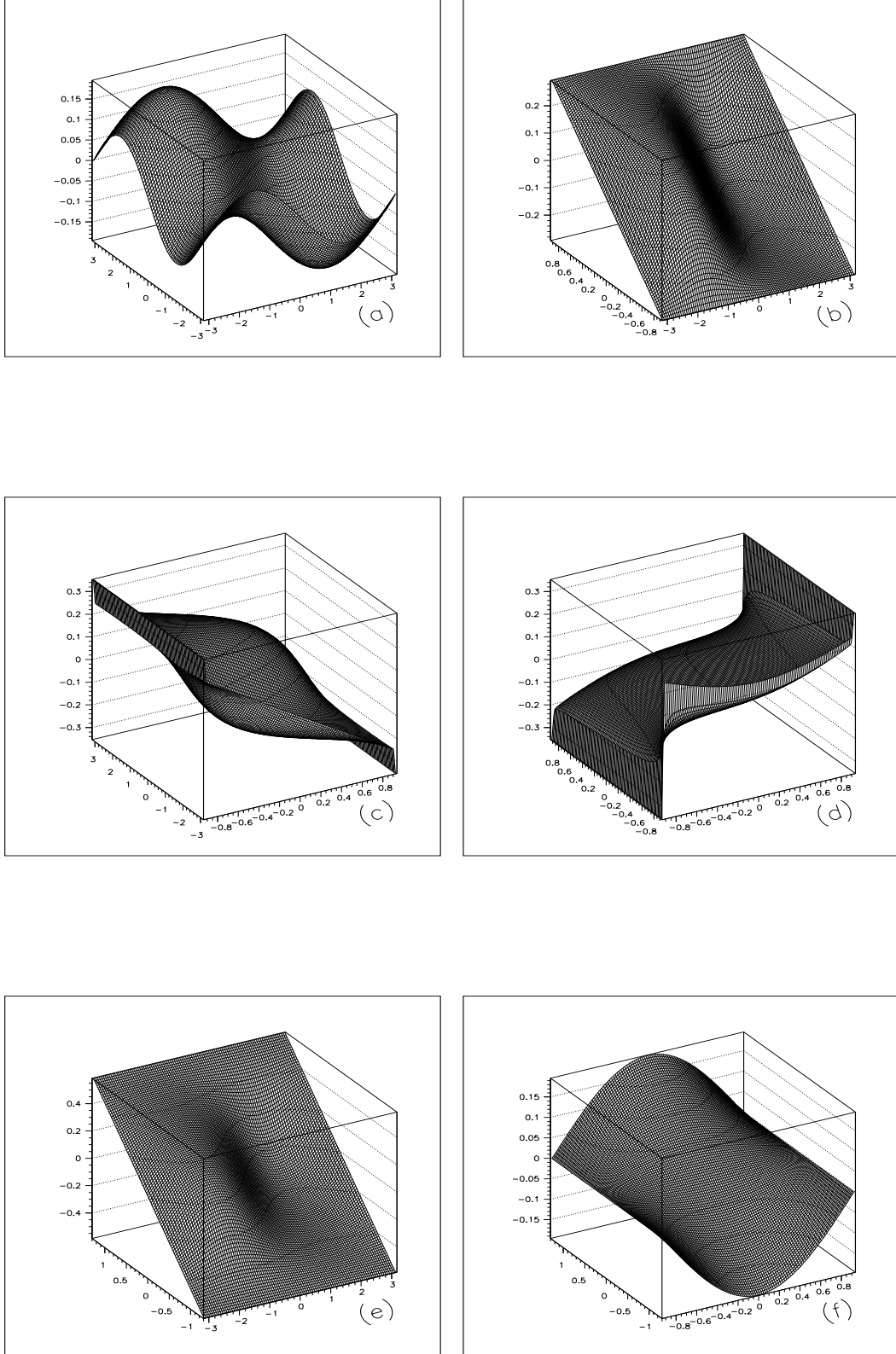


FIG. 7: The two-pseudofermion phase-shift expansions (64)-(69) for (a) $\Phi_{c0,c0}(q, q')$, (b) $\Phi_{c0,s1}(q, q')$, (c) $\Phi_{s1,c0}(q, q')$, (d) $\Phi_{s1,s1}(q, q')$, (e) $\Phi_{c0,c1}(q, q')$, and (f) $\Phi_{s1,c0}(q, q')$, respectively, as a function of q and q' for $n = 0.59$ and $U/t = 4.9$.

which again is the correct result. In the limit $U/t \rightarrow 0$, the $c0, \iota', \iota''$ branch lines disappear, all spectral weight being transferred over to the $s1$ branch line, which becomes the non-interacting removal electron spectrum. As the limits $U/t \rightarrow 0$ and $U/t \rightarrow \infty$ are approached, the exponent (31) tends to the following values,

$$\zeta_{c0, \iota', \iota''}(q) = -\frac{\iota' \iota''}{\sqrt{2}} + \frac{1}{2}; \quad U/t \rightarrow 0; \quad \zeta_{c0, \iota', \iota''}(q) = -\frac{\iota' \iota''}{2} + \frac{1}{8}; \quad U/t \rightarrow \infty, \quad (72)$$

for the q and k values of the spectral-function expression (30). Thus, in the limit $U/t \rightarrow 0$, it is given by $-1/\sqrt{2} + 1/2$ for the branch lines such that $\iota' \iota'' = 1$ and $1/\sqrt{2} + 1/2$ for the branch lines such that $\iota' \iota'' = -1$. Furthermore, for $U/t \rightarrow \infty$ the exponent is given by $-3/8$ for the branch lines such that $\iota' \iota'' = 1$ and $5/8$ for the branch lines such that $\iota' \iota'' = -1$.

Thus, for the momentum domain such that $-k_F < k < k_F$, the PDT provides the correct $U/t = 0$ one-electron removal spectral distribution. Moreover, our $U/t \rightarrow \infty$ expressions of Eqs. (70) and (72) agree with the results obtained by the method of Refs. [10, 11, 12], as mentioned above.

Let us now consider the LHB one-electron addition branch lines. For the spectral-function expression (34) the multiplicative function $C_{s1, \iota'}^i(k)$ is such that $C_{s1, \iota'}^i(k) \rightarrow 0$ as $U/t \rightarrow 0$. Thus, the $s1, \iota'$ branch lines disappear at $U/t = 0$, which is the correct result. In the limits $U/t \rightarrow 0$ and $U/t \rightarrow \infty$, we find the following expressions for the $m \rightarrow 0$ exponent (35),

$$\zeta_{s1, \iota'}^i(q) = 1; \quad U/t \rightarrow 0; \quad \zeta_{s1, \iota'}^i(q) = -\frac{q}{2k_F} \left(\iota' - \frac{q}{4k_F} \right); \quad U/t \rightarrow \infty. \quad (73)$$

These expressions are valid for the q and k values of the the spectral-function expression (34). In the limit $U/t \rightarrow \infty$, this exponent is $\zeta_{s1, \iota'}^i(q) = -3/8$ for $q \rightarrow \iota' k_F$, $\zeta_{s1, \iota'}^i(q) = 0$ for $q = 0$, and $\zeta_{s1, \iota'}^i(q) = 5/8$ for $q \rightarrow -\iota' k_F$.

For the LHB one-electron addition branch line (38), the multiplicative function $C_{c0, \iota''}^i(q)$ gives rise to the finite weight constant $(1/N_a)^{\zeta_0(q)} \rightarrow 1$ of the δ -peak spectral-function expression of Eq. (14) for the two branch line sectors such that $\iota'' = \text{sgn}(k)1$. In contrast, that function vanishes for the other two branch line sectors such that $\iota'' = -\text{sgn}(k)1$. As further discussed below, the $c0, \iota''$ branch lines such that $\text{sgn}(k) \iota'' = 1$ give rise to the correct $U/t = 0$ one-electron removal spectrum for momentum values k in the range $k_F < |k| < [\pi - k_F]$. In contrast, the two $c0, \iota''$ branch lines such that $\text{sgn}(k) \iota'' = -1$ disappear as $U/t \rightarrow 0$, which again is the correct result. We also find that in the limits $U/t \rightarrow 0$ and $U/t \rightarrow \infty$ and for $m \rightarrow 0$, the exponent (39) reads,

$$\zeta_{c0, \iota''}^i(q) = -\text{sgn}(q) \iota''; \quad 2k_F < |q| \leq \pi; \quad U/t \rightarrow 0; \quad \zeta_{c0, \iota''}^i(q) = -\frac{3}{8}; \quad 2k_F < |q| \leq \pi; \quad U/t \rightarrow \infty. \quad (74)$$

Thus, in the limit $U/t \rightarrow 0$, this exponent is given by -1 and 1 for $\text{sgn}(q) \iota'' = 1$ and $\text{sgn}(q) \iota'' = -1$, respectively. The expressions of Eq. (74) are valid for the q and k values of the spectral-function expression (38).

We emphasize that in the $m \rightarrow 0$ limit and for momentum values $k_F < |k| \leq [\pi - k_F]$, the two $c0, \iota''$ branch line sectors such that $\text{sgn}(k) \iota'' = 1$ give rise to the $U/t = 0$ non-interacting electronic spectrum in the limit $U/t \rightarrow 0$. In such a limit, the exponent (39) becomes -1 for all values of q , as confirmed by Eq. (74). Thus, the spectral function behaves as given in the second expression of Eq. (38). According to Eq. (A1) of Ref. [16] with $c \equiv c0$, in the limit $U/t \rightarrow 0$ and for momentum values such that $k_F < |k| \leq [\pi - k_F]$, the dispersion $\epsilon_{c0}(\iota'' k_F + k)$ becomes, for $\text{sgn}(k) \iota'' = 1$, the electronic spectrum $-2t[\cos(k) - \cos(k_F)]$. Thus, combination of the one-electron removal $s1$ branch line for $|k| < k_F$ with the present two LHB one-electron addition $c0, \iota''$ branch line sectors such that $\text{sgn}(k) \iota'' = 1$ for $k_F < |k| < [\pi - k_F]$ recovers the non-interacting electronic spectrum in the limit $U/t \rightarrow 0$.

Finally, let us consider the UHB one-electron addition problem. For the UHB one-electron addition branch line expression (41), the multiplicative function $C_{s1_u}^i(q)$ gives rise for $U/t \rightarrow 0$ to the finite weight constant $(1/N_a)^{\zeta_0(q)} \rightarrow 1$ of the δ -peak spectral-function expression of Eq. (14). Moreover, according to Eq. (A2) of Ref. [16], in the limit $U/t \rightarrow 0$, the dispersion $\epsilon_{s1}(\pi - k)$ becomes the $U/t = 0$ electronic spectrum for $\pi - k_F \leq |k| \leq \pi$. We recall that the energy pseudogap $\Delta_{UHB-LHB}$ given in Eq. (42) vanishes as $U/t \rightarrow 0$ for all values of the electronic density n . Consistently, according to Eq. (70), the UHB exponent $\zeta_{s1_u}(q)$ is given by $\zeta_{s1_u}(q) = -1$ as $U/t \rightarrow 0$ for all values of q and momentum k of the spectral function expression (44). Thus, following the second expression of Eq. (41), the correct non-interacting electronic spectral function is reached in this limit.

On the other hand, for the UHB one-electron addition branch line expression (44), the multiplicative function is such that $C_{s1_u, \iota'}^i(q)$ vanishes as $U/t \rightarrow 0$. The same occurs for the corresponding multiplicative functions of the UHB one-electron addition branch line expressions (46) and (49), which are such that $C_{c^u, \iota', \iota''}^i(q)$ and $C_{c1, \iota', \iota''}^i(q)$ vanish as $U/t \rightarrow 0$. Again this is the correct result, since the corresponding branch lines do not exist at $U/t = 0$. Furthermore,

we find that the limiting values of the $m \rightarrow 0$ exponent (50) of the UHB one-electron addition branch line expression (49) are the following,

$$\zeta_{c1, \iota', \iota''}^i(q) = -\frac{1}{4} \left(1 - [2\iota' + \iota'' - \text{sgn}(q) 2]^2 \right); \quad U/t \rightarrow 0; \quad \zeta_{c1, \iota', \iota''}^i(q) = \frac{1}{2} \left(\iota' + \frac{\iota''}{2} - \frac{q}{[\pi - 2k_F]} \right)^2; \quad U/t \rightarrow \infty, \quad (75)$$

for the q and k values of that expression. Then, in the limit $U/t \rightarrow 0$, the exponent is given by $\zeta_{c1, \iota', \iota''}^i(q) = 0$ for $\text{sgn}(q) \iota' = 1$, $\zeta_{c1, \iota', \iota''}^i(q) = 2$ for $\text{sgn}(q) \iota' = \iota' \iota'' = -1$, and $\zeta_{c1, \iota', \iota''}^i(q) = 6$ for $\text{sgn}(q) \iota' = -\iota' \iota'' = -1$. On the other hand, for $U/t \rightarrow \infty$ and $\iota' \iota'' = -1$ the exponent is such that $1/8 \leq \zeta_{t, \iota', \iota''}^i(q) < 9/8$, whereas for $\iota' \iota'' = 1$ it has the range $1/8 < \zeta_{t, \iota', \iota''}^i(q) < 25/8$.

We found above that the one-electron $s1$ branch line becomes the non-interacting electronic spectrum for the removal part of the spectrum, which corresponds to $-k_F < k < k_F$. Also the $c0, \iota'$ branch line sectors of the LHB one-electron addition spectrum such that $\iota' = \text{sgn}(k)$, become the addition non-interacting spectrum for momentum values $k_F < |k| \leq [\pi - k_F]$. Thus, if we combine these results with the $s1_u$ branch line of the UHB one-electron addition spectrum for $[\pi - k_F] < |k| \leq \pi$ and the vanishing of the energy pseudogap $\Delta_{UHB-LHB}$ as $U/t \rightarrow 0$, one finds that the one-electron addition non-interacting spectrum is reached as $U/t \rightarrow 0$ for the whole momentum domain such that $k_F < |k| < \pi$. It follows that the correct $U/t = 0$ spectra are reached as $U/t \rightarrow 0$ both for the one-electron removal and the one-electron addition momentum domains such that $0 < |k| < k_F$ and $k_F < |k| < \pi$, respectively.

On the other hand, for finite values of U/t , the spectral weight spreads over a larger two-dimensional region of the (k, ω) -plane. However, most of the spectral weight is located in the vicinity of separated and independent $c0$, $s1$, and $c1$ branch lines and of the envelope line considered in Sec. V. At half-filling this occurs for the $c0$ and $s1$ branch lines only and there is no LHB. Our study provides the momentum and energy dependence of the weight distribution in the vicinity of such $\alpha\nu$ branch lines for both the one-electron removal and addition spectral weight distributions. In the $m \rightarrow 0$ limit, the maximum spread of the one-electron spectral-weight distribution occurs for $U/t \rightarrow \infty$, where the problem had been already studied in Refs. [10, 11, 12]. The $U/t \rightarrow \infty$ maximum spreading of the one-electron removal and LHB addition spectral weight at electronic density $n = 1/2$ is illustrated in Fig. 1 of Ref. [11] for the spectral functions $B^{-1}(k, \omega)$ and $B_1^{+1}(k, \omega)$, respectively. (These functions are called $B(k, \omega)$ and $A(k, \omega)$, respectively, in that article.)

V. COMMENTS ABOUT THE RELATION TO THE PHOTOEMISSION DISPERSIONS OF TTF-TCNQ

An interesting realization of a quasi-1D metal is the organic charge-transfer salt TTF-TCNQ [1, 4]. The experimental dispersions in the electron removal spectrum of this quasi-1D conductor as measured by ARPES are shown in Fig. 9 (b) of Ref. [4] and Fig. 4 of Ref. [22]. The experimental data in these figures were taken with He I radiation (21.2 eV) at a sample temperature of 60 K on a clean surface obtained by *in situ* cleavage of a single crystal. Instrumental energy and momentum resolution amounted to 70 meV and 0.07 \AA^{-1} , respectively.

We note that the low-energy spectral properties of TTF-TCNQ involve inter-chain hopping and electron-phonon interactions. Thus, the 1D Hubbard model PDT results are to be applied above the energies of these processes. The singular branch lines studied in Sec. III correspond to (k, ω) -plane regions where there are one-electron spectral-weight singular features. While it is difficult to measure the exponents experimentally, a crucial test for the suitability of the model (1) to describe real quasi-1D materials is whether the ARPES peak dispersions correspond to the singular branch lines and other divergent spectral features predicted by the PDT of Refs. [18, 19].

The electronic density of TCNQ is $n = 0.59 < 1$. For densities in the domain $0 < n < 1$ and one-electron removal, all singular spectral features predicted by the general PDT are of branch line type. Thus, for TCNQ all divergent spectral features correspond to the singular branch lines studied in Sec. III. While the theoretical weight-distribution branch-line expressions of that section refer to all values of U/t and n , a detailed study of the spectral-function k, ω , and U/t dependence in the vicinity of the branch lines obtained in this paper confirms the validity of the preliminary predictions of Refs. [4, 22]: the electron removal spectra calculated for $t = 0.4 \text{ eV}$, $U = 1.96 \text{ eV}$ ($U/t = 4.90$), and $n = 0.59$ yields an almost perfect agreement with the three TCNQ experimental dispersions. The exception is the low-energy behavior, as a result of the inter-chain hopping and electron-phonon interactions, as mentioned above. If accounted for a renormalization of the transfer integral due to a possible surface relaxation [1], these values are in good agreement with estimates from other experiments [2, 3].

The experimental TCNQ finite-energy peak dispersions of Fig. 4 of Ref. [22] correspond to the spin $s \equiv s1$ branch line (20) and charge $c \equiv c0, +1, +1$ and $c' \equiv c0, -1, -1$ branch lines (28) of Fig. 1. Those are the only finite-weight singular branch lines in the one-electron removal spectral function for $U/t = 4.90$ and $n = 0.59$. Importantly, only these singular branch lines, whose line shape is controlled by negative exponents, lead to TCNQ peak dispersions

in the real experiment. The exponent (23) corresponds to the spin $s \equiv s1$ branch line and is plotted in Fig. 2 for $0 < k < k_F$. The exponents (31) that correspond to the charge $c \equiv c0, +1, +1$ branch line and charge $c' \equiv c0, -1, -1$ branch line are plotted in Figs. 3 and 4, respectively. As reported in Sec. III, for finite values of U/t the value of the constant $C_{c0, -1, -1}(q)$ of the spectral-function expression (30) strongly decreases for momentum values such that $2k_F < k < 3k_F$. This is consistent with the absence of TCNQ experimental spectral features for momentum values $k > 0.59\pi \approx 0.50 \text{ \AA}^{-1}$ in Fig. 4 of Ref. [22], along the corresponding $c' \equiv c0, -1, -1$ branch line of Fig. 1.

Thus, our detailed branch-line PDT analysis fully agrees with the preliminary theoretical results of Refs. [4, 22] for the TCNQ problem. On the other hand, the theoretical predictions of the TTF dispersions presented in Ref. [22] are very preliminary. While most singular power-law spectral features are of branch line type, there is a second type of such features which correspond to some of the border lines introduced in Ref. [19]. For the electronic density value corresponding to the TCNQ stacks the main singular spectral features are of branch-line type. In contrast, a careful analysis of the problem by means of the general PDT reveals that for the electronic density suitable to the TTF stacks the singular features are both of branch-line and border-line type. Once the preliminary studies of TTF presented in Ref. [22] involve the singular branch line features only, a very small value of U is predicted. However, if instead one takes into account all singular features provided by the PDT, the best quantitative agreement with the TTF experimental dispersions is reached for larger values of U/t , as confirmed elsewhere.

VI. DISCUSSION AND CONCLUDING REMARKS

In this paper we have used the exact PDT of Refs. [18, 19] to study the energy and momentum dependence of the one-electron spectral weight distribution in the vicinity of the singular and edge branch lines of the 1D Hubbard model. A careful and detailed analysis of the spectral function expressions in the proximity of the branch lines obtained here confirms the validity of the preliminary theoretical predictions of Refs. [4, 22], in what the description of the band TCNQ dispersions observed by ARPES in the quasi-1D organic compound TTF-TCNQ is concerned. Indeed, the use of the spectral function expressions derived here confirms that in contrast to the conventional band structure description [4], the singular branch lines and other divergent features obtained from the 1D Hubbard model describe quantitatively, for the whole finite-energy band width, the peak dispersions observed in that compound. For the TCNQ band, the 1D Hubbard model description assumes an electronic density of $n = 0.59$ and yields best agreement with experiment for $U/t = 4.9$.

The TCNQ conduction band displays spectroscopic signatures of spin-charge separation on an energy scale of the band width. This seems to indicate that the dominant non-perturbative many-electron microscopic processes studied in Refs. [18, 19] by means of the PDT and the associated scattering mechanisms investigated in Refs. [20, 21] control the unusual finite-energy spectral properties of TTF-TCNQ. The quantitative agreement for the whole finite-energy band width between the 1D Hubbard model PDT theoretically predicted spectral features and the TCNQ photoemission dispersions of TTF-TCNQ reveals that for finite-energy the local effects of the Coulomb electronic correlations fully control the spectral properties of that material. Thus, we expect that the long-range Coulomb interactions, disorder, and impurity effects play very little role in the finite-energy and/or finite-temperature properties of TTF-TCNQ. That disorder and impurities do not play a major role is confirmed by the occurrence of charge-spin separation for the whole energy band width.

We emphasize that our present finite-energy description goes beyond the usual low-energy investigations by means of bosonization [8] and conformal-field theory [9]. For low-energy the present quantum problem is a TTL. This concept only applies to the low-energy parts of the one-electron spectrum of Fig. 1, where the spectral dispersions can be linearized. However, our results refer to all values of the group velocities associated with the branch lines plotted in these figures. Thus, the spin-charge separation found here for the whole energy band width is not associated with the usual TTL behavior, which refers to low energy only. Moreover, only our finite-energy theoretical spectral features describe the experimental TCNQ dispersions of TTF-TCNQ. Indeed, the low-energy TTL linear part of the one-electron spectrum plotted in Fig. 1 has no physical significance for that quasi-1D compound, since the low-energy spectral properties of TTF-TCNQ involve inter-chain hopping and electron-phonon interactions. Thus, for the present TCNQ photoemission problem, the 1D physics described by the 1D Hubbard model only becomes experimentally relevant for finite energy, where the low-energy TTL description does not apply.

This paper is an extension of some of the preliminary results about the momentum and energy dependence of the one-electron spectral function of the model in the vicinity of the singular and edge branch lines presented in short form in Ref. [22]. More recently, a study of the same problem by DDMRG calculations reached similar results [23]. A detailed theoretical study of the the TTF experimental dispersions by means of the PDT, including consideration of both singular branch lines studied here and singular border lines is in progress and will be presented elsewhere. Moreover, the calculation of the one-electron spectral-function of the 1D Hubbard model for all values of k and ω by use of the general PDT is also in progress. Finally, our results are of interest for the understanding of the

spectral properties of the new quantum systems described by cold fermionic atoms on an optical lattice: Following the experimental studies of strongly correlated quantum systems of ultra cold bosonic atoms held in optical lattices [33], new experiments involving cold fermionic atoms [such as ^6Li] on an optical lattice formed by interfering laser fields are in progress.

Acknowledgments

We thank A. Bjelis, A. Castro Neto, F. Guinea, E. Jeckelmann, P. A. Lee, J. M. B. Lopes dos Santos, L. M. Martelo, J. P. Pouget, M. Sing, and U. Schwingenschlögl for stimulating discussions. J.M.P.C and K.P. thank the financial support of the EU money Center of Excellence ICA1-CT-2000-70029, J.M.P.C. and D.B. the hospitality and support of MIT, J.M.P.C. thanks the financial support of the Calouste Gulbenkian Foundation and Fulbright Commission, K.P. the financial support of the OTKA grant T049607, D.B. the financial support of FCT grant SFRH/BD/6930/2001 and the hospitality of Research Institute for Solid State Physics and Optics in Budapest, and R.C. the financial support of Deutsche Forschungsgemeinschaft (CL 124/3-3 and SFB 484).

-
- [1] R. Claessen, M. Sing, U. Schwingenschlögl, P. Blaha, M. Dressel, and C. S. Jacobsen, Phys. Rev. Lett. **88**, 096402 (2002).
 - [2] F. Zwick, D. Jérôme, G. Margaritondo, M. Onellion, J. Voit, and M. Grioni, Phys. Rev. Lett. **81**, 2974 (1998).
 - [3] S. Kagoshima, H. Nagasawa, and T. Sambongi, *One-dimensional conductors* (Springer, Berlin, 1987), and references therein.
 - [4] M. Sing, U. Schwingenschlögl, R. Claessen, P. Blaha, J. M. P. Carmelo, L. M. Martelo, P. D. Sacramento, M. Dressel, and C. S. Jacobsen, Phys. Rev. B **68**, 125111 (2003).
 - [5] Elliott H. Lieb and F. Y. Wu, Phys. Rev. Lett. **20**, 1445 (1968); P. B. Ramos and M. J. Martins, J. Phys. A **30**, L195 (1997); M. J. Martins and P.B. Ramos, Nucl. Phys. B **522**, 413 (1998).
 - [6] M. Takahashi, Prog. Theor. Phys. **47**, 69 (1972).
 - [7] B.D. Simons, P.A. Lee, and B.L. Altshuler, Phys. Rev. Lett. **70**, 4122 (1993); M. Arikawa, Y. Saiga, and Y. Kuramoto, Phys. Rev. Lett. **86**, 3096 (2001); Karlo Penc and B. Sriram Shastry, Phys. Rev. B **65**, 155110 (2002); M. Arikawa, T. Yamamoto, Y. Saiga, and Y. Kuramoto, Nucl. Phys. B **702** (2004) 380.
 - [8] H. J. Schulz, Phys. Rev. Lett. **64**, 2831 (1990).
 - [9] Holger Frahm and V. E. Korepin, Phys. Rev. B **43**, 5653 (1991) and references therein.
 - [10] Karlo Penc, Frédéric Mila, and Hiroyuki Shiba, Phys. Rev. Lett. **75**, 894 (1995);
 - [11] Karlo Penc, Karen Hallberg, Frédéric Mila, and Hiroyuki Shiba, Phys. Rev. Lett. **77**, 1390 (1996).
 - [12] Karlo Penc, Karen Hallberg, Frédéric Mila, and Hiroyuki Shiba, Phys. Rev. B **55**, 15 475 (1997).
 - [13] S. Sorella and A. Parola, Phys. Rev. Lett. **76**, 4604 (1996).
 - [14] D. Sénéchal, D. Perez, and M. Pioro-Ladrière, Phys. Rev. Lett. **84**, 522 (2000).
 - [15] J. M. P. Carmelo, J. M. Román, and K. Penc, Nucl. Phys. B **683**, 387 (2004).
 - [16] J. M. P. Carmelo and P. D. Sacramento, Phys. Rev. B **68**, 085104 (2003).
 - [17] J. M. P. Carmelo, cond-mat/0405411.
 - [18] J. M. P. Carmelo and K. Penc, cond-mat/0311075.
 - [19] J. M. P. Carmelo and K. Penc, preprint.
 - [20] J. M. P. Carmelo, cond-mat/0504271.
 - [21] J. M. P. Carmelo, D. Bozi, and P. D. Sacramento, unpublished.
 - [22] J. M. P. Carmelo, K. Penc, L. M. Martelo, P. D. Sacramento, J. M. B. Lopes dos Santos, R. Claessen, M. Sing, and U. Schwingenschlögl, Europhys. Lett. **67**, 233 (2004).
 - [23] H. Benthien, F. Gebhard, and E. Jeckelmann, Phys. Rev. Lett. **92**, 256401 (2004).
 - [24] J. M. P. Carmelo, F. Guinea, K. Penc, and P. D. Sacramento, Europhys. Lett. **68**, 839 (2004).
 - [25] J. M. P. Carmelo and K. Penc, preprint.
 - [26] J. M. P. Carmelo, P. Horsch, and A. A. Ovchinnikov, Phys. Rev. B **45**, 7899 (1992).
 - [27] J. M. P. Carmelo, L. M. Martelo, and P. D. Sacramento, J. Phys.: Cond. Matt. **16**, 1375 (2004).
 - [28] J.M.P. Carmelo, F. Guinea, and P.D. Sacramento, Phys. Rev. B **55**, 7565 (1997).
 - [29] T. Takahashi *et al.*, J. Phys. C: Solid State Phys. **17**, 3777 (1984).
 - [30] J. P. Pouget, in *Semiconductors and Semimetals*, Vol. **37**, 87, ed. by E. Conwell (Academic Press, New York, 1988).
 - [31] S. Yunoki, T. Tohyama, and S. Maekawa, Physica B **230-232**, 1050 (1997).
 - [32] J. M. P. Carmelo, K. Penc, and P. D. Sacramento, unpublished.
 - [33] M. Greiner, O. Mandel, T. Esslinger, T. W. Hänsch, and I. Bloch, Nature **415**, 39 (2002); B. Paredes, A. Widera, V. Murg, O. Mandel, S. Fölling, I. Cirac, G. V. Shlyapnikov, T. W. Hänsch, and I. Bloch, Nature **429**, 277 (2004).